Study on proton conduction in *N*-methylimidazole and acetic acid equimolar mixture liquid

N-メチルイミダゾール－酢酸等量混合液体の

プロトン伝導に関する研究

Hiroyuki Doi

Graduate School of Science and Technology

Niigata University

TABLE OF CONTENTS

Chapter 1
INTRODUCTION

1-1. Ion conduction in solution

In 1883, S. Arrhenius proposed “the theory of electrolytic dissociation”. In this theory, it is proposed that salt in solution dissociates into the ionic species of A^+ and B^- and these species contribute to electric conduction as it is shown as following.[1] And it has been believed in general for years that salt dissociates in solution to contribute to electric conduction.

$$\mathbf{AB \rightarrow A^+ + B^-} \quad (1\text{-}1)$$

In terms of kinetics of solute in aqueous solution, several kinds of empirical equation and relationship were provided, stokes law (1-2) and Walden rule (1-3), which is known as the proportional relationship between infinite molar ionic conductivity λ_i and viscosity η, Stokes-Einstein equation (1-4), which is defined as the relationship between diffusion coefficient D and viscosity coefficient η, and Nernst-Einstein equation (1-5), which is defined as the relationship between molar ionic conductivity Λ and diffusion coefficient D. All of the relationship and equation are given as following.

$$\lambda_i^{\infty}\eta = \frac{z_i^2 F^2}{k'\pi N_A r_i} \left(k' = 6 \text{ or } 4\right) \quad (1\text{-}2)$$

where z_i is electric charge of ion, F is drag force of the fluid on a sphere, k' is parameter of boundary condition, N_A is Avogadro's number, r_i is radius of the sphere. The right side of the equation is constant in infinite dilution condition.

$$\lambda_i^{\infty}\eta = \text{constant} \quad (1\text{-}3)$$

$$D = \frac{kT}{c\pi\eta r_s} \quad (1\text{-}4)$$

where k is Boltzmann constant, T is absolute temperature, c is

concentration of the solute in solution, and r_i is radius of the sphere.

$$\Lambda = \frac{N_A e^2}{k_B T}\left(D^+ + D^-\right) \quad (1\text{-}5)$$

where e is elementary charge, D^+ and D^- is diffusion coefficient of cation and anion species. These empirical equation and relationship are widely used for clarifying the kinetics of the mobile ions in the aqueous solutions.

And besides, these equation and relationship have been applied even for that of the mobile ions in non-aqueous solutions despite that all of these equation and relationship are empirical equation and relationship which are provided in aqueous solution.

On the other hand, as far as I have been reseached the paper, in 1888, third generation of non-solvent molecular liquids which is composed only of ionic species could be found[2] and such a kind of liquids have become somewhat of a worldwide phenomenon since the mid-1990s when the concept of using a "molten salt" as a solvent became widely publicized.

1-2. History of ionic liquid

Around 1970's, with the intensive research of Ionic liquid, the term of "ionic liquid" was established and the ionic liquid was defined as the liquid which has a melting point or glass-transition temperature below 100 degree Celsius and is composed only of the ionic species of cation B^+ and anion A^- in the liquid.[3] Room-temperature ionic liquids have attracted remarkable attention as new materials for various chemical applications.[4]

In 1914, Walden et al. reported novel protic ionic liquid of ethylammonium nitrate EAN and reported the physicochemical properties of EAN, which has a low melting point of 14 ◦C. EAN attracts remarkable attention for its unique properties today, however EAN has not received much attention at that time.[4]

In 1900's, several ionic liquids which are composed of $[(AlCl_3)Cl]^-$ anion were reported. However, such ionic liquids had a disadvantage of a low stability in air and moisture.

Then, in 1992, Wilkes et al. reported 1-ethyl-3-methylimidazolium tetrafluoroborate ionic liquid which has a high stability in air and moisture and was water-soluble ionic liquid.[5]

1-ethyl-3-methylimidazolium tetrafluoroborate ionic liquid had a high concentration of ionic species per unit volumes, therefore this Wilkes's report[5] triggered a rapid increase of the research of the ionic liquids as not only the electrolyte but also high thermal stability, catalysts for various organic reactions and so on. In 2003, Watanabe et al. reported imidazolium bis(trifluoromethanesulfonyl)amide as proton-conducting nonaqueous electrolytes. and Angell et al. also reported protic ionic liquids as proton-conducting nonaqueous electrolytes.[6, 7]

1-3. Classification of ionic liquid

In 2012, Angell et al. classified the ionic liquid into four kinds of categories; Aprotic ionic liquids, Protic ionic liquids, Inorganic ionic liquids, and Solvate (chelate) Ionic liquids.[8]

First of all, Aprotic ionic liquids are the liquids which do not have a dissociable hydrogen atom in the liquids; e.g. ethylpyridinium bromide and aluminum chloride.[9]

Second, Protic ionic liquids $[HB^+][A^-]$ are the liquids which have a dissociable hydrogen atom in the liquids, in which HB^+ and A^- stand for the conjugated cation and anion of a Brønsted base B and acid HA. Protic ionic liquids can be simply prepared with mixing HA and B to yield onium salts $[HB^+][A^-]$ by proton transfer.[10-12]

The auto-protolysis equilibrium from HB^+ to A^- in protic ionic liquids is given as following. (1-6)

$$HB^+ + A^- \leftrightarrow HA + B \quad K_S = [HA][B] \quad (1\text{-}6)$$

where K_S is auto-protolysis constant in protic ionic liquids.

The physicochemical properties of protic ionic liquids have been predicated by ab initio calculations[13], and properties such as viscosity, ionic conductivity, thermal properties, liquid surface tension and refractive index experimentally investigated[14-18]. Various solvent parameters[19, 20] and

Hammett acidity function[21-23] have been evaluated. Protic ionic liquids offer their unique properties that make them attractive to a broad field of applications, such as new proton transfer materials for fuel cells[24,25] catalysts or solvents for organic syntheses[26] and so on.

Third, Inorganic ionic liquids are the liquids which are composed only of inorganic compounds; e.g. lithium perchlorate $LiClO_3$.[8]

Last, Solvate (chelate) Ionic liquids are the liquids which are composed of multivalent cation; e.g. calcium nitrate tetrahydrate $Ca(NO_3)\bullet 4H_2O$.[27]

1-4. Intermolecular interaction in ionic liquids

It is generally known that the solvent physicochemical and acid-base properties vary on cation and anion species changing and ion-ion interactions in the liquid.

Angell et al. discussed the intermolecular or ion-ion interaction in protic ionic liquids in terms of the relationship between excess boiling point ΔT_b and ΔpK_a,[28] where ΔT_b is the deviation of the experimental value of boiling point and the average between the boiling point of acid and base, where both of acid and base are the compounds which composes protic ionic liquids. For this purpose, ΔpK_a[29] is defined as $\Delta pK_a = pK_a(HB^+) - pK_a(HA)$, where $pK_a(HB^+)$ and $pK_a(HA)$ represent negative value of common logarithms of the acid dissociation constant for B and HA in aqueous solution, respectively. Also, definition of ΔT_b is described as following.

Among the series of several protic liquids reported in this paper, it was revealed that it shows a good linear relationship between ΔT_b and ΔpK_a.

The mixtures of the series of protic liquids have positive ΔT_b values because it exist intermolecular interaction or ion-ion interaction in the mixture. Thus, amplitudes of the ΔT_b of the series of the protic ionic liquids can be described as they reflect the intermolecular or ion-ion interaction in protic ionic liquids. And besides, according to the paper, it shows a good linear relationship between ΔT_b and ΔpK_a, it can be described that ΔpK_a value also reflects the intermolecular or ion-ion interaction in protic ionic liquids.

In this paper, Angell et al. concluded that the protic liquids, which have a low ΔpK_a value, compose low concentration of ionic species in the liquids, therefore such a protic ionic liquids show low ionic conductivity.

However, when the concentration of the ionic species in the liquids is low, the intermolecular or ion-ion interaction in protic ionic liquids also should be small. Therefore, molar ionic conductivity in the mixture should be high on the contrary to Angell et al.'s conclusion. Also, it can be also a problem to discuss the intermolecular or ion-ion interaction in ionic liquid by means of ΔpK_a, which is qualitative value from aqueous solution.

1-5. Angell's classification of ion conduction in ionic liquids

On the basis of Walden rule, Angell et al. classified the ionic conductive behavior in the ionic liquids by means of Walden plot, which is a double logarithmic plot between molar ionic conductivity and reciprocal viscosity.[7, 29]

Angell et al. suggest that it can be classified the ionic conductive behavior of the liquid by the ideal Walden line in Walden plot, and this line which has a slope of 1 straight is plotted for the purpose of criterion assuming that the constant of Walden rule as 1. Therefore, when the ionic species in the liquid flow ideally according to the Walden rule, the plot will lie on the ideal Walden line. Actual ideal Walden line is plotted by 1 mol dm^{-3} KCl aqueous solution which shows similar behavior of ideal Walden line.[7]

Angell et al. proposed that the liquid which is plotted above the ideal Walden line, the liquid shows a specific ionic conductive behavior as the liquid has a higher ionic conductivity in comparison to the viscosity which is expected from the ionic conductivity on the basis of Walden rule. Angell et al. classified such a liquid as *superionic* liquid. On the other hand, Angell et al. also proposed that the liquid which is plotted beneath the ideal Walden line, the liquid shows a low ionic conductive behavior as the liquid has a lower ionic conductivity in comparison to the viscosity which is expected from the ionic conductivity on the basis of Walden rule. Angell et al. classified such a liquid as *poorionic* liquid.

However, as it was discussed in the previous section, when the concentration of the ionic species in the liquids is low, the intermolecular or ion-ion interaction in protic ionic liquids also should be small. Therefore, molar ionic conductivity in the mixture should be high on the contrary to Angell et al.'s classification.

To sum up, it can be necessary to determine the concentration of ion species in protic ionic liquids and to plot the Walden plot by actual molar conductivity of the protic ionic liquid for evaluating such a "*poorionic* liquid" to whether "*superionic*" liquid or "*poorionic*" liquid.

1-6. Purpose of this study

As is discussed above, ion conduction in the solution has a long history, and the emerge of the ionic liquid which it is classified into four kinds of ionic liquids have been attracted remarkable attention as new proton materials for fuel cells, catalysts for organic syntheses and solvents for reactions and so on. Also, Solvent physicochemical and acid-base properties of ionic liquids play an important role in these applications.

In addition, from both of the discussion of the Angell's conclusion about the intermolecular or ion-ion interaction in ionic liquid and the Angell's classification of the ionic conductive behavior in ionic liquid, it was suggested that it can be necessary to determine the concentration of ion species in protic ionic liquids and to plot the Walden plot by actual molar conductivity of the protic ionic liquid for evaluating such a "*poorionic* liquid" to whether "*superionic*" liquid or "*poorionic*" liquid.

Firstly, *N*-alkylimidazolium based protic ionic liquids are one of the most well known protic ionic liquids. In particular, physicochemical properties of *N*-methylimidazolium based protic ionic liquids are widely investigated before. Therefore, we investigated a series of protic ionic liquids made from *N*-methylimidazole and five acids with a wide variety of acidities from strong acids to weak ones.

In **Chapter 3**, the acidity of trifluoromethansulfonic acid, bis(trifluoromethanesulfonyl)amide, trifluoroacetic acid, formic acid and

acetic acid in *N*-methylimidazolium based protic ionic liquids was discussed by means of direct potentiometric and calorimetric titrations.

In **Chapter 4**, we focused the attention into the ionic conductive behavior of *N*-methylimidazole C_1Im equimolar mixture with acetic acid AcOH, and for further insight into ion-conductive behavior of the C_1Im and AcOH equimolar mixture, Raman spectroscopic study with the aid of quantum calculations was performed, and ionic conductivity, viscosity, and density were measured at various temperatures.

1-7. References

1. S. A. Arrhenius, *Doctoral thesis*, **1883**
2. Gabriel, S. Et al., *Ber. der Deutschen Chem. Ges.*, **1888**, *21*, 2669–2679.
3. Freemantle, M. *An Introduction to Ionic Liquids; Royal Society of Chemisty, Cambridge, UK*, **2010**.
4. M. Armand et al., *Nat.Mater.* **2009**, *8*, 621 –629.
5. J. S. Wilkes et al., *Chem. Soc., Chem. Commun.*, **1992**, 965.
6. M. Watanabe et al., *J. Phys. Chem. B*, **2003**, *107*, 4024-4033
7. C. A. Angell, *Science*, **2003**, *302*, 5644, 422-425
8. C. A. Angell et al., *Faraday Discuss.*, **2012**, *154*, 9–27
9. F. H. Hurley and T. P. Wier, *J. Electrochem. Soc.*, **1951**, *98*, 203.
10. Hirao, M.; Sugimoto, H.; Ohno, H. *J. Electrochem. Soc.* **2000**, *147*, 4168.
11. Yoshizawa, M.; Ogihara, W.; Ohno, H. *Electrochem. Solid-State Lett.* **2001**, *4*, E25.
12. Ohno, H.; Yoshizawa, M. *Solid State Ionics* **2002**, *154-155*, 303.
13. Markusson, H.; Belieres, J-P.; Johansson, P.; Angell, C. A.; Jacobsson, P. *J. Phys. Chem. A* **2007**, *111*, 8717.
14. Xu, W.; Angell, C. A. *Science* **2003**, *302*, 422.
15. Evans, D. F.; Yamauchi, A.; Roman, R. ; Casassa, E. Z. *J. Colloid Interface Sci.* **1982**, *88*, 89.
16. Shetty, P. H.; Youngberg, P. J. Kersten, B. R.; Poole, C. F. *J. Chromatogr.* **1987**, *411*, 61.

17. Greaves, T. L.; Weerawardena, A.; Fong, C.; Krodkiewska, I.; Drummond, C. J. *J. Phys. Chem. B* **2006**, *110*, 22479.
18. Belieres, J-P.; Angell, C. A. *J. Phys. Chem. B* **2007**, *111*, 4926.
19. Shetty, P. H.; Youngberg, P. J. Kersten, B. R.; Poole, C. F. *J. Chromatogr.* **1987**, *411*, 61.
20. Poole, S. K. Shetty, P. H.; Poole, C. F. *Anal. Chim. Acta.* **1989**, *218*, 241.
21. Thomazeau, C.; Olivier-Bourbigou, H.; Magna, L.; Luts, S.; Gilbert, B. *J. Am. Chem. Soc.* **2003**, *125*, 5264.
22. Robert, T.; Olivier-Bourbigou, H.; Magna, L.; Gilbert, B. *ECS Trans.* **2007**, *3*, 71.
23. Robert, T.; Magna, L.; Olivier-Bourbigou, H.; Gilbert, B. *J. Electrochem. Soc.* **2009**, *156*, F115.
24. Susan, M. A. B. H.; Noda, A.; Mitsushima, S.; Watanabe, M. *Chem. Commun.* **2003**, 938.
25. Noda, A.; Susan, M. A. B. H.; Kudo, K.; Mitsushima, S.; Hayamizu, K.; Watanabe, M. *J. Phys. Chem. B* **2003**, *107*, 4024.
26. Welton, T. *Chem. Rev.* **1999**, *99*, 2071.
27. C. A. Angell, *J. Electrochem. Soc.*, **1965**, *112*, 1224.
28. M. Yoshizawa, W. Xu, C. A. Angell, *J. Am. Chem. Soc.*, **2003**, *125*, 15411-15419
29. Yoshizawa, M.; Xu, W.; Angell, C. A. *J. Am. Chem. Soc.*, **2003**,*125*, 15411−15419.

Chapter 2

EXPERIMENTAL

2-1. Materials

Ionic liquid

All sample ionic liquids used in this study were dried in a vacuum desiccator over P_2O_5 for more then 72 h, stored in a dry argon-filled glove box. The water content was less than 100 ppm in all the systems according to a Karl Fischer method before measurements. The product purity was also checked with elemental analysis. Detailed information was also shown in respective Chapters.

Syntheses of *N*-methylimidazolium based protic ionic liquid

C_1Im was used after distillation under reduced pressure. Liquid acids, TfOH, trifluoroacetic acid, acetic acid, and formic acid, were purified by distillation. Tf_2NH was used without further purification. C_1Im was added by driblets into an aqueous solution containing equimolar HA in an ice bath. The prepared compounds were dried in vacuo for several weeks at room temperature. The water contents of these final products were determined by the Karl Fisher method to be typically less than 1 mol % (400 ppm). The elemental analyses suggest negligible impurities perturbing the target acid−base reaction. Density of the sample liquid was measured using a vibration tube densimeter (Kyoto Electronics, DA-310) above the melting point.

1-methylimidazole equimolar mixture with acetic acid

C_1Im and AcOH were dried over a molecular sieve 4Å for several weeks, and then each was distilled under reduced and ambient pressure, respectively. Equivalent amount of each liquid was mixed with a gradual droplet addition of the acid to the base avoiding vaporization by generation of the heat of mixing. Purity and a water content of the final equimolar mixture were checked by elemental analysis and the Karl-Fischer titration,

respectively. All chemicals were treated and stored in a glove box, in which a water content was kept less than 1 ppm.

2-2. Measurements

Potentiometric Titration

A sample of 4−6 g was set into a glass vessel with a water jacket in which the thermostatted fluid was circulated. Then the temperature was elevated to melt solid samples and thermostatted at 325 K (Tf_2NH-C_1Im), 367 K (TfOH-C_1Im), or 338 K (CF_3COOH-C_1Im) within a temperature fluctuation of 0.01 K. A known amount of the corresponding HA is added to prepare an acidic solution into the sample. A Pt(H_2) electrode was immersed into the sample solution. An Ag/AgCl reference electrode was separated from the sample with a double-junction salt bridge. The cell for emf (electromotive force) measurement is represented as: Ag/AgCl | 0.1 mol dm−3 NaCl (aq) || CH_3COOH + C_1Im || sample solution | Pt(H_2). The reference electrode was kept at room temperature (298 K) except for the immersed tip in the sample. To achieve stable emf measurement, various salt bridges were tested. Finally, we found that the CH_3COOH + C_1Im equimolar mixture was the best among others, thus, it was used as a salt bridge in common, though contamination from the bridge may occur to some extent. A more adequate salt bridge is needed for more accurate and stable emf measurements in PIL solutions, as well as those in aqueous ones.[1] Hydrogen gas was bubbled in the sample. After the equilibrium emf was attained, the sample was directly titrated by liquid C_1Im in the vessel. The cell showed quick response (<5 min for stabilization) and gave satisfactorily stable emf ($3\sigma < 0.1$ mV) in each titration point except for around the neutralization point.

Calorimetric Titration.

Calorimetric measurements were carried out for the liquid samples at 298 K (HA = CH_3COOH or HCOOH). Fully automatic titration and data acquisition system with a twin-type isoperibol calorimeter (Tokyo Riko, Co.

Ltd.) was used. A liquid C_1Im or HA-C_1Im mixture (30 cm^3) was placed in a Teflon vessel inserted in a thermostatted aluminum block at 25 ± 0.1 °C with a fluctuation ±0.0001 °C in an air bath. In the vessel, aliquots of HA were added from an autoburet (APB-510, Kyoto Electronics) and the heats generated were determined from the temperature profile detected by doubled thermistors in the vessels on the basis of Newton's law of cooling. The thermal conductivity in Newton's law and the heat capacity of the cell were calibrated at each titration point with known Joule heat generated by a standard resistance. The titrations of the opposite direction (C_1Im added into a neat HA or a mixture) were also carried out through the entire composition range. The measured heats ranged from 0 to 45 J, with an average 3σ of 0.4 J.

Raman spectroscopies

Raman spectra were obtained using an FT-Raman spectrometer (Perkin-Elmer GX-R) equipped with a Nd:YAG laser operating at 1064 nm. The laser power was kept at 800 mW throughout the measurements. The optical resolution was 2.0 cm^{-1}, and spectral data were accumulated 512 times to obtain data of a sufficiently high signal-to-noise ratio. Temperature varying Raman measurements were carried out with a hermetically sealed quartz cell whose temperature fluctuation was kept within ±0.3 K at a given temperature during the measurement. The sample room was filled with dry nitrogen gas to avoid condensation of moisture on the surface of the Raman cell at low temperature. Raw Raman spectra were corrected in terms of solution densities, which had been measured in advance, and were normalized based on the adequate Raman band. The densities of the sample solutions were measured using a vibrating-tube-based density meter (Kyoto Electronics DA-300).

By using thus corrected Raman intensity $I(\nu)$, Raman spectra are represented as a form of the reduced Raman intensity $R(\nu)$ given as follows;

$$R(\nu) \equiv I(\nu)(\nu_0 - \nu)^{-4}\,\nu[1 - \exp(-hc\nu/kT)] \qquad (2\text{-}3),$$

where ν_0 and ν cm^{-1} represent the frequencies of the irradiated laser light and Raman shift, respectively, and the others are physical constants or quantities of usual meanings. $R(\nu)$ spectra were then deconvoluted into single component of a pseudo-Voigt function.

The viscosity, ion conductivity and density mesurements

Ionic conductivity was measured with ALS/H Instruments model 604C electrochemical analyzer. Viscosity was measured with Lauda iVisc and Brookfield DV-II+ Pro viscometers calibrated with glycol aqueous solutions at various temperatures. Density was measured with a KEK DA-310 vibration tube density-meter after calibration with dried air and degassed water at each temperature. All measurements were carried out within temperature fluctuation of ±0.1 K at a given temperature.

2-3. Computational calculation.

Molecular Orbital Calculations

Quantum calculations were carried out for an isolated molecules, ions and ion pairs (finally molecular complexes) in gas phase at the B3LYP/6-311+G(d,p) level of theory. Basis set superposition error (BSSE) was corrected by a counterpoise method. Polarizable continuum model (PCM) was used for the calculations in acetonitrile. In the PCM calculations, atomic radii including a hydrogen atom were explicitly considered by using those in the UFF force fields. For the species in dielectric solutions, the BSSE correction was also estimated with single point calculations in gas phase at the optimized geometry in solutions. Normal vibration analysis was performed for all of the species at the optimized geometries except scanning potential energy surfaces to confirm they have no imaginary frequency. *Gaussian03* program suite was used for all quantum chemical calculations. [2]

2-4. References

1. Kakiuchi, T. J. *Solid State Electrochem.* **2011**, *15*, 1661−1671. Sakaida, H.; Kakiuchi, T. *J. Phys. Chem. B* **2011**, *115*, 13222−13226. Kakiuchi, T.; Yoshimatsu, T.; Nishi, N. *Anal. Chem.* **2007**, *79*, 7187−7191.
2. M. J. Frisch, G. W. Trucks, H. B. Schlegel, G. E. Scuseria, M. A. Robb, J. R. Cheeseman, J. A. Montgomery Jr, T. Vreven, K. N. Kudin, J. C. Burant, J. M. Millam, S. S. Iyengar, J. Tomasi, V. Barone, B. Mennucci, M. Cossi, G. Scalmani, N. Rega, G. A. Petersson, H. Nakatsuji, M. Hada, M. Ehara, K. Toyota, R. Fukuda, J. Hasegawa, M. Ishida, T. Nakajima, Y. Honda, O. Kitao, H. Nakai, M. Klene, X. Li, J. E. Knox, H. P. Hratchian, J. B. Cross, V. Bakken, C. Adamo, J. Jaramillo, R. Gomperts, R. E. Stratmann, O. Yazyev, A. J. Austin, R. Cammi, C. Pomelli, J. W. Ochterski, P. Y. Ayala, K. Morokuma, G. A. Voth, P. Salvador, J. J. Dannenberg, V. G. Zakrzewski, S. Dapprich, A. D. Daniels, M. C. Strain, O. Farkas, D. K. Malick, A. D. Rabuck, K. Raghavachari, J. B. Foresman, J. V. Ortiz, Q. Cui, A. G. Baboul, S. Clifford, J. Cioslowski, B. B. Stefanov, G. Liu, A. Liashenko, P. Piskorz, I. Komaromi, R. L. Martin, D. J. Fox, T. Keith, M. A. Al-Laham, C. Y. Peng, A. Nanayakkara, M. Challacombe, P. M. W. Gill, B. Johnson, W. Chen, M. W. Wong, C. Gonzalez, J. A. Pople, GAUSSIAN 03, Revision D.01, Gaussian, Inc., Wallingford CT, 2004.

Chapter 3

Acid−Base Property of *N*-Methylimidazolium-Based Protic Ionic Liquids Depending on Anion

3-1. INTRODUCTION

Protic ionic liquids (PILs) are a subclass of room-temperature ionic liquids (RTILs) and are composed of onium salts. Ethanolammonium nitrate[1] and ethylammonium nitrate[2] (EAN) have been reported to be molten salts at room temperature, and currently they are recognized to be typical PILs. PILs are made with neutralization of a Brønsted acid HA and a base B.

$$\mathbf{HA} + \mathbf{B} \rightarrow \mathbf{A}^- + \mathbf{HB}^+ \quad (1)$$

Nowadays, various PILs of wide-ranging cation and anion are available.[3–6] Because of a dissociable hydrogen on the onium cation, PILs are expected as new solvents for acid−base reaction media[7–10] and as proton conductors in fuel cells.[11–15] In many cases, strong acids are chosen for a proton source of PILs. As the acidity of any strong acids in a solution is leveled by the conjugate acid of the solvent, one of the features of PILs is that the strong acid HA must exist as an acidic form in acidic PILs. Thus, the proton donating ability of HA in PILs has a significant meaning in PILs' chemistry as acid−base reaction media. Hence, the efforts have been made to clarify the acid− base property of PILs. We can find typical work of spectroscopy quantifying the PILs acidity by using solvatochromic dyes.[16] Gilbert et al. have shown the acidity level of various acids in several protic/aprotic ionic liquids by evaluating Hammet
acidity function H_0.[17,18] They proposed the acidity order of HPF_6 > HBF_4 > Tf_2NH > TfOH (Tf_2N^- = bis-(trifluoromethanesulfonyl)amide, TfO^- = trifluoromethanesulfonate), which agrees well with the tendency in the gas phase acidity.[19,20] Direct measurement approaching pK_a of some bases in RTILs have been carried out by Barhdadi et al.[21] Owing to the proton

donating and accepting abilities of HB^+ and A^-, respectively, PILs are considered as amphoteric solvents. In this context, the following equilibrium corresponds to an autoprotolysis, which is practically a characteristic reaction in amphoteric solvents.

$$\mathbf{HB^+ + A^- \rightarrow HA + B} \quad (2)$$

The products HA and B are, respectively, the conjugate acid and base of the solvent ionic species, and hence, are the practical proton donating and accepting species in PILs. If we consider a PIL as an amphoteric solvent, the equilibrium constant K_S = [HA][B] (square brackets are used for representing the species molarity as an ordinary way throughout this paper) corresponds to an autoprotolysis constant, from which a degree of ionization by reaction 1 is estimated. And also, as is well established, K_S is a parameter concerning with acid−base properties such as a pH-window and a pH-scale.[22] Although one of the best ways to evaluate K_S is direct pH measurement, it is quite difficult because a usual glass electrode is practically unavailable in PILs. For an alternative of K_S, Angell et al. have proposed an index $\Delta \mathrm{p}K_a$,[23] or a "proton free energy level"[24,25] for PILs. They have defined $\Delta \mathrm{p}K_a$ as $\Delta \mathrm{p}K_a = \mathrm{p}K_a(HB^+) - \mathrm{p}K_a(HA) = -\log[HA][B]/[HB^+][A^-]$, where $\mathrm{p}K_a(HB^+)$ and $\mathrm{p}K_a(HA)$ represent the respective acid dissociation constants of HB^+ and HA in an aqueous phase. It has been demonstrated that $\Delta \mathrm{p}K_a$ is relevant to the predicted boiling points of PILs that may reflect an ionic character of PILs.[23] MacFarlane et al., have also shown a relationship between $\Delta \mathrm{p}K_a$ and 1H NMR chemical shift of the *N*-methyl group in a series of *N*-methylpyrrolidinium-based PILs.[3] Bautista-Martinez et al., have also shown a parameter ΔV_{gap}, a potential gap between acidic and basic saturated conditions in PILs determined by cyclic voltammetry, and they found a positive correlation between ΔV_{gap} and $\Delta \mathrm{p}K_a$.[26] However, it is well-known that the $\mathrm{p}K_a$ values considerably depend on the solvent because the solvation free energy is frequently comparable to the gas phase acidity itself, especially in the

charged species such as HB^+ or A^-. In addition, when HA is a strong acid, it is impossible to evaluate the essential pK_a values in an aqueous phase due to the leveling effect. Hence, it can be said that ΔpK_a is clearly distinguishable from pK_S (= −log K_S). Recently, we demonstrated the direct pH measurement in EAN and its aqueous mixtures, and have successfully determined pK_S value of EAN with appropriate electrodes such as Pt(H_2) and the IS-FET (ion selective field effect transistor).[27,28] In fact, the pK_S value 9.83 is significantly different from ΔpK_a of 12.0. Moreover, the reaction entropy of autoprotolysis in EAN is large and positive, while the corresponding reaction entropy in water is large and negative.[29] The fact suggests that reaction entropy for the autoprotolysis plays completely different role in PILs and molecular liquids; that is, it enhances autoprotolysis in Gibbs free energy in PILs, while it reduces in molecular solvents. Thus, pK_S is an essential thermodynamic quantity of PILs, even though ΔpK_a is practically useful as a measure of the acid−base property of the PIL without direct measurements. In the present study, to shed more light to the solvent acid− base nature of PILs, we investigated a series of PILs made from *N*-methylimidazole (C_1Im) and five acids with a wide variety of acidities from strong acids to weak ones by direct potentiometric and calorimetric titrations. We demonstrated that the acidity of two widely used strong acids, TfOH and Tf_2NH, are practically similar in these PILs, and that the acidity of trifluoroacetic acid is much weaker than TfOH and Tf_2NH. In addition, we found that the mixtures of C_1Im and acetic acid and formic acid are not essentially ionic liquids.

3-2. EXPERIMENTAL

3-2-1. Materials

Methylimidazole (Nippon Synthetic Chemical Industry, >99.99%) was used after distillation under reduced pressure. Liquid acids, TfOH (Central Glass, >99.5%), trifluoroacetic acid (Kishida Chemical, 99%), acetic acid (Kishida Chemical, 99.7%), and formic acid (Kishida Chemical, >98%),

were purified by distillation. Tf_2NH (Morita Chemical Industries) was used without further purification. C_1Im was added by driblets into an aqueous solution containing equimolar HA in an ice bath. The prepared compounds were dried in vacuo for several weeks at room temperature. The water contents of these final products were determined by the Karl Fisher method to be typically less than 1 mol % (400 ppm). The elemental analyses suggest negligible impurities perturbing the target acid−base reaction. Density of the sample liquid was measured using a vibration tube densimeter (Kyoto Electronics, DA-310) at the temperature of carrying out potentiometric titration.

3-2-2. Potentiometric Titration.

A sample of 4−6 g was set into a glass vessel with a water jacket in which the thermostatted fluid was circulated. Then the temperature was elevated to melt solid samples and thermostatted at 325 K (Tf_2NH-C_1Im), 367 K (TfOH-C_1Im), or 338 K (CF_3COOH-C_1Im) within a temperature fluctuation of 0.01 K. A known amount of the corresponding HA is added to prepare an acidic solution into the sample. A Pt(H_2) electrode was immersed into the sample solution. An Ag/AgCl reference electrode was separated from the sample with a double-junction salt bridge. The cell for emf (electromotive force) measurement is represented as: Ag/AgCl | 0.1 mol dm−3 NaCl (aq) || CH_3COOH + C_1Im || sample solution | Pt(H_2). The reference electrode was kept at room temperature (298 K) except for the immersed tip in the sample. To achieve stable emf measurement, various salt bridges were tested. Finally, we found that the CH_3COOH + C_1Im equimolar mixture was the best among others, thus, it was used as a salt bridge in common, though contamination from the bridge may occur to some extent. A more adequate salt bridge is needed for more accurate and stable emf measurements in PIL solutions, as well as those in aqueous ones.[30] Hydrogen gas was bubbled in the sample. After the equilibrium emf was attained, the sample was directly titrated by liquid C_1Im in the vessel. The cell showed quick response (<5 min for stabilization) and gave

satisfactorily stable emf ($3\sigma < 0.1$ mV) in each titration point except for around the neutralization point.

3-2-2. Calorimetric Titration.

Calorimetric measurements were carried out for the liquid samples at 298 K (HA = CH_3COOH or HCOOH). Fully automatic titration and data acquisition system with a twin-type isoperibol calorimeter (Tokyo Riko, Co. Ltd.) was used. A liquid C_1Im or HA-C_1Im mixture (30 cm^3) was placed in a Teflon vessel inserted in a thermostatted aluminum block at 25 ± 0.1 °C with a fluctuation ±0.0001 °C in an air bath. In the vessel, aliquots of HA were added from an autoburet (APB-510, Kyoto Electronics) and the heats generated were determined from the temperature profile detected by doubled thermistors in the vessels on the basis of Newton's law of cooling. The thermal conductivity in Newton's law and the heat capacity of the cell were calibrated at each titration point with known Joule heat generated by a standard resistance. The titrations of the opposite direction (C_1Im added into a neat HA or a mixture) were also carried out through the entire composition range. The measured heats ranged from 0 to 45 J, with an average 3σ of 0.4 J.

3-3. RESULT AND DISCUSSION

Strong Acids.

As the H_0 value of pure TfOH is much more negative (−14.1[31−33] or −13[34]) than pure H_2SO_4, TfOH is a widely used superacid as a proton donating compound for acidcatalyzed reactions. Tf_2NH has attracted attention as its stronger gas-phase acidity than TfOH.[19,20] However, the acidity order of the two acids is ambiguous because it depends on the solvent.[35,36] In some cases, much more negative pK_a of TfOH (actually H_0) than that of Tf_2NH (~−4) has been employed.[3,23,33] We compare here the acidity by directly observed K_S in the PILs of common base. Figure 1 shows potentiometric titration curves in $C_1hIm^+A^-$ (A^- = Tf_2N^- or TfO^-). Δ_{cH} represents the excess molarity of acid species HA; Δ_{cH} = [HA] − [C_1Im]. As described in

the Experimental Section, initially acidic solutions containing excess acid (Δ_cH > 0) were titrated with C_1Im. By adding a titrant, the emf was gradually decreased with decreasing Δ_cH and suddenly dropped at around the equivalence point ([HA] = [C_1Im]). Then, it slowly decreased again by further addition of C_1Im. This observation indicates that the Pt(H_2) electrode responds to [HA] in both PILs. The obtained neutralization curves may be likely to usual ones observed in aqueous solutions, suggesting that the equilibrium of autoprotolysis should be established in these PILs. The large emf jumps indicate that both PILs have rather large pK_S values. If we assume a Nernstian response of the Pt electrode to [HA] in the PILs, the observed emf E_i at the i-th titration point can be represented as

$$\boldsymbol{E_i = E^{o'} + 2.303RT / F \log[HA]_i} \quad (3)$$

where $E^{\circ\prime}$ and T denote the apparent standard potential of the cell and temperature, respectively. $E^{\circ\prime}$ is a constant involving the activity coefficient of acid in the PIL, γ_H. Supposing that K_S = [HA][C_1Im] holds, [HA] can be calculated from K_S and Δ_cH at each titration point. It should be noted that to prepare completely neutral PILs is practically impossible, so that the excess acid (either positive or negative) in the prepared sample PIL δ_{HA} have to be taken into consideration of Δ_cH. Thus, $E°$ and pK_S, as well as δ_{HA}, are optimized to minimize the error square sum $U = \Sigma(E_{i,obs} - E_{i,calc})^2$ in which $E_{i,obs}$ and $E_{i,calc}$ stand for the calculated and observed emfs in the i-th titration point, respectively. Finally, obtained values are listed in Table 1, and the calculated curves, using the refined values, are shown with solid lines in Figure 1. As it can be seen in this figure, the calculated curves reproduce well each series of experimental points; therefore, the respective pK_S value can be satisfactorily determined. According to the evaluated pK_S value in $C_1hIm^+Tf_2N^-$, the concentrations of neutral species, [Tf_2NH] and [C_1Im], can be estimated to be 5.1×10^{-5} M (M = mol dm^{-3}) at the equivalence point (Δ_cH = 0). On the other hand, the concentrations of ions,

[C_1hIm^+] and [Tf_2N^-], are practically equal to c_{PIL} = 1000d/MW, where d and MW are the density of the PIL and the formula weight of $C_1hIm^+Tf_2N^-$, respectively. The c_{PIL} value is 4.9 M; thus, the ionic species evidently exist in much excess than the neutral species. Similarly, [TfOH] = [C_1Im] = 3.4 × 10^{-5} M in $C_1hIm^+TfO^-$ at Δ_{cH} = 0, where c_{PIL} (= [C_1hIm^+] = [TfO^-]) = 5.8 M. Consequently, it can be said that the equimolar mixtures of these strong acids and C_1Im almost completely consist of ions in practical means.

Potentiometric Titrations in PILs of Weak Acids.

Although CF_3COOH is classified as a weak acid due to a positive pK_a (0.5), CF_3COOH is acidic enough to be almost completely dissociated in an aqueous solution. The potentiometric titration curve in $C_1hIm^+CF_3COO^-$ is shown in Figure 2. An emf jump observed at the neutralization point means the mixture mostly composed of C_1hIm^+ and CF_3COO^-. However, in comparison with $C_1hIm^+TfO^-$ and $C_1hIm^+Tf_2N^-$, the emf drop was more moderate or much C_1Im was required to invert from acidic to basic solution; this indicates much more neutral species exist at an equivalence point than those in $C_1hIm^+TfO^-$ or $C_1hIm^+Tf_2N^-$. Thus, as the significant amount of neutral species coexists, the theoretical curve in Figure 2 drawn with a solid line was calculated by using $K_S^* = x_{HA} \cdot x_{C1Im}/(x_A \cdot x_{C1hIm})$, instead of K_S, and $E = E^{\circ\prime *} + 2.303\ F/RT(\log x_{HA}, ic_{PIL})$, where x_j denotes the molar fraction of component j (j = HA, C_1Im, A^-, and C_1hIm^+, A^- = CF_3COO^-). K_S^* and $E^{\circ\prime *}$ were then obtained similarly by minimizing U. $E^{\circ\prime *}$ is different definition from $E^{\circ\prime}$ in the strict sense, while the $E^{\circ\prime *}$ value can be numerically compared with $E^{\circ\prime}$. For the purpose of comparison, K_S^* is converted to pK_S by pK_S = −log K_S^* − 2 log c_{PIL}. The final values are listed in Table 1. As shown, pK_S for $C_1hIm^+CF_3COO^-$ are significantly smaller than those for PILs consisting of strong acids. The concentrations of neutral species at Δ_{cH} = 0 are calculated by using K_S^* to be 0.036 M. Although this value is much larger than that for $HMm^+Tf_2N^-$ and $C_1hIm^+TfO^-$ the ionic species are still much excess (c_{PIL} = 6.9 M) over the neutral species in $C_1hIm^+CF_3COO^-$, and hence, the equimolar mixture

practically consists of ions. The smaller pK_S value than that in $HMm^+Tf_2N^-$ and $C_1hIm^+TfO^-$ indicates the proton donating ability of CF_3COOH in $C_1hIm^+CF_3COO^-$ is obviously much weaker than that of Tf_2NH and TfOH. CH_3COOH and HCOOH are much weaker acids than CF_3COOH in an aqueous phase. In a dilute aqueous solution of equimolar CH_3COOH and C_1Im, according to pK_as, 94% of either is ionized to form CH_3COO^- and C_1hIm^+, respectively. However, as shown in Figure 2, no practical emf jump near the equivalence point was observed in the potentiometric titrations, which indicates the proton transferred ionic species is never predominant and neutral species may considerably exist. Depending on the medium, some proton transfer patterns from CH_3COOH to C_1Im have been proposed. In nonpolar solvents such as chloroform, an incomplete proton transfer and a hydrogen-bonding adduct formation like $CH_3COO^-\cdots H^+\cdots C_1Im$ has been suggested.[37,38] In a vapor phase at a higher temperature, a hydrogen-bonded $CH_3COOH\cdots C_1Im$ was proved by Raman spectroscopy.[39] According to ab initio calculations, the potential energy surface of H^+ between imidazole-N and O of CH_3COO^- was revealed to depend on the dielectric constant, that is, H^+−N distance of 1.05−1.1 Å is a single potential well in a gas phase while another potential well at H^+−O distance of 1−1.05 Å appears in a medium of higher dielectric constants.[40] All of these facts strongly support our findings.

Calorimetric Titrations in PILs of Weak Acids.

In the mixtures of C_1Im and weak acids (HA = CH_3COOH or HCOOH) calorimetric titrations have been carried out. The heat generated by adding aliquots of HA or C_1Im to the solution successively, q_{add} was recorded at an each titration point. Figure 3 shows the apparent molar reaction enthalpy defined as $\Delta H_{app}^{\circ} = -q_{add}/m_{add}$ as a function of the molar ratio of C_1Im in the mixture after each addition of the titrant x_{C1Im}, where m_{add} is the number of moles of HA or C_1Im added at an each titration point. At the beginning of addition of C_1Im into HA (shown with the closed squares in Figure 3), the ΔH_{app}° was significantly large and negative for both CH_3COOH and

HCOOH. The extrapolated value of ΔH_{app} toward $x_{C1Im} = 0$, $\Delta H_{app,0}$ was −43 kJ/mol for CH_3COOH and −69 kJ/mol for HCOOH, respectively. ΔH_{app}° was then increased immediately with increasing x_{C1Im}, and approached to zero at around $x_{C1Im} = 0.5$ via the value of $\Delta H_{app,0}^{\circ}/2$ at around $x_{C1Im} = 0.25$. On the other hand, ΔH_{app}° for addition of CH_3COOH into C_1Im (shown with the open squares in Figure 3) at $x_{C1Im} = 1$ was about −10 kJ/mol. ΔH_{app}° was then kept almost unchanged down to $x_{C1Im} = 0.5$, then increased to reach zero with decreasing x_{C1Im}. The ΔH_{app}° value for the addition of HCOOH at $x_{C1Im} > 0.5$ was rather scattered, probably due to a decarbonylation and a decarboxylation of HCOOH.[41] We, thus, no longer discuss about the results of HCOOH titration into C_1Im. $\Delta H_{app,0}^{\circ}$ for CH_3COOH was 26 kJ/mol less negative than $\Delta H_{app,0}^{\circ}$ for HCOOH. This gap in $\Delta H_{app,0}^{\circ}$ is greater than that in their dissociation enthalpies in water; small and similar values of ±1 kJ/mol have been reported for both CH_3COOH and HCOOH.[42] We can consider that the addition of a small amount of C_1Im into neat HA involves the following processes: (1) isolation of monomeric HA and C_1Im as possible reactants into the gas phase, (2) proton transfer reaction from HA to C_1Im in the gas phase, and (3) solvation of the possible products of A^- and C_1hIm^+ by neat HA. The enthalpic cost for process (1) of HCOOH is rather larger relative to that of CH_3COOH due to a larger heat of vaporization and cohesive energy density.[43] From the gas phase experiments, the difference between CH_3COOH and HCOOH in the dissociation enthalpies (5.9 kJ/mol[44]) are much smaller than the gap in $\Delta H_{app,0}^{\circ}$. Therefore, the unexpectedly larger $\Delta H_{app,0}^{\circ}$ for CH_3COOH than that for HCOOH should be associated with process (3). That is, HCOOH has a significantly large dielectric constant in comparison to CH_3COOH, owing to a large dipole moment, and has large solvation energy for the charged solutes, so that process (3) is enthalpically more favorable in HCOOH than in a less polar CH_3COOH. Similarly, $\Delta H_{app,1}^{\circ}$ represents the extrapolated ΔH_{app}° value at $x_{C1Im} = 1$ in the titration of CH_3COOH into neat C_1Im. Comparing $\Delta H_{app,1}^{\circ}$ with $\Delta H_{app,0}^{\circ}$ for CH_3COOH−C_1Im system, $\Delta H_{app,1}^{\circ}$ was significantly less negative than

$\Delta H_{app,0}^{\circ}$. We can also consider the respective processes (1−3) corresponding to those mentioned above. If we assume that the same proton transfer reaction occurs in both titrations, independent from the titration direction, the processes (1) and (2) are common. It should be noted that process (3) involves cavity formation to embed solutes. CH_3COOH is a highly ordered solvent of hydrogen bonding. Nishi et al. revealed CH_3COOH is an associated liquid, mainly due to the chain-like self-association.[45−48] On the other hand, $C_1Im\cdots C_1Im$ interaction should arise from dipole−dipole interaction. In fact, endothermic mixing of C_1Im and nonpolar solvents such as normal alkanes has also been reported.[49,50] The experimental fact that $\Delta H_{app,1}^{\circ}$ was significantly less negative than $\Delta H_{app,0}^{\circ}$. This suggests that larger endothermic enthalpy for the cavity formation in neat C_1Im than that in neat CH_3COOH and solvation by C_1Im to the product ions is significantly weaker than that by CH_3COOH. Possible interpretation may be that the hydrogen bonding among the solvent CH_3COOH molecules is kept both in the cavity formation and in the solvation in neat CH_3COOH. For more detailed discussion, however, spectroscopic investigations are needed. In the middle composition range, one of the common features of the titration curves given in ΔH_{app}° is that it becomes the value of $\Delta H_{app,0}^{\circ}/2$ or $\Delta H_{app,1}^{\circ}/2$ at $x_{C1Im} < 0.5$. In these ranges of solvent composition, the heat of mixing also significantly contributes in ΔH_{app}°. We depict the calorimetric titration data in excess enthalpy of mixing, H^E ($H^E = \Sigma q_{mix}/\Sigma m_j$). As shown in Figure 4, the titration curves evaluated with a different titration direction were practically the same with each other, which suggest that no hysteretic behavior was found in calorimetric titrations. Therefore, all the processes involved in the mixing should be fast, and the species distribution in the mixture never depends on titration direction but only on the solvent composition. As clearly shown in Figure 4, the H^E curves are asymmetric with a minimum of 7.3−7.4 kJ/mol at x_{C1Im} = 0.30−0.32. It indicates that stoichiometric aggregates or adducts seems to be formed in the mixture. In addition, the minimum at x_{C1Im} = 0.30−0.32 suggests that an adduct formation of C_1Im:CH_3COOH = 1:2. Similar results have also been

reported in mixtures of C_2H_5COOH−triethylamine[51] and CH_3COOH−*N*-methylpyrrolidine.[52] In such mixtures, the transport properties, such as viscosity and ionic conductivity, show a maximum at the component of carboxylic acids excess region. Orzechowski et al., have proposed an adduct formation of C_2H_5COOH:triethylamine = 2:1, together with a 1:1 hydrogen-bonding adduct and dissociated free ionic species.[51] The minimum H^E value was about −13 kJ/mol at about $x_{triethylamine}$ = 0.33. Less negative H^E for CH_3COOH−C_1Im than that for C_2H_5COOH−triethylamine implies that CH_3COO^- and C_1hIm^+ may not exist as free ions, but hydrogen bonding adducts should be plausibly formed also in CH_3COOH−C_1Im mixture, and the bonding energy is smaller than those formed in C_2H_5COOH−triethylamine. In addition, according to ab initio calculation in a gas phase, the stabilization energy of $CH_3COOH\cdots C_1Im$ hydrogen-bonding adduct formation is 53.46 kJ/mol.[39] Finally, we discuss titration curves in ΔH_{app}° here again to estimate the ionization ratio (or degree of proton transfer) from the calorimetric data. As aforementioned, titration curve for C_1Im titration into the acids approached zero in ΔH_{app}° at around x_{C1Im} = 0.5, while the titration curve of the inverted direction converged to zero at x_{C1Im} = 0.2. The latter suggests that heat, except the proton transfer reaction, such as the heat of mixing and dilution, considerably contributes in ΔH_{app}°. Therefore, we discuss only the calorimetric titration curves for C_1Im titration into the acids. We first consider calorimetric titration curves for simple strong acid and base neutralization. In this case, the values in ΔH_{app}° should be kept constant until the equivalence point, and then they suddenly turn off (go to zero) at the equivalence point. Typical titration curves for such strong acid and base titration are shown by a dashed line in Figure 3. It should be noted that the constant ΔH_{app}° values until the equivalence point equal to the proton transfer enthalpy for the strong acid and base. Here, let us compare the titration curves for C_1Im and CH_3COOH or HCOOH systems with those for simple strong acid and base neutralization. ΔH_{app}° for C_1Im and CH_3COOH or HCOOH are always less negative than the dashed line at the

composition range below the equivalence point, indicating that C_1Im protonation may partially occur in the mixture. The protonation ratio of C_1Im is defined by $\alpha_{C1Im} = m_{C1hIm}/(m_{C1hIm} + m_{C1Im})$, where m_j is the number of moles of respective species *j* in the mixture. If we assume the observed heat contains only that for the proton transfer reaction α_{C1Im} could be estimated from the total heat generated until the titration point, as follows:

$$\alpha_{C1Im} = \frac{\int_0^{x_{C1Im}} \Delta H_{app}{}^{o} \mathrm{d}x_{C1Im}}{x_{C1Im} \Delta H_{app,0}{}^{o}} \quad (4)$$

Based on eq 4, α_{C1Im} at x_{C1Im} = 0.5 is estimated to be 0.43 for CH_3COOH-C_1Im and 0.45 for HCOOH-C_1Im. The formally obtained pK_S values from $K_S = \{(1 - \alpha_{C1Im})\, c_{PIL}\}^2$ are −1.3 for CH_3COOH−C_1Im and −1.4 for HCOOH−C_1Im, respectively. The values are similar with each other despite a significantly different $\Delta H_{app,0}{}^{\circ}$ and ΔpK_a in an aqueous phase. Although such an estimation is rather rough, however, it is worth pointing out that, at most, a half of C_1Im or some extent is proton attached to be ionized in the equimolar mixtures of CH_3COOH or HCOOH.

Acid−Base Property of the PILs.

The pK_S values generally corresponds the practical pH-range (0 to pK_S) for the respective solvent. Figure 5 represents the pH range or a pH-window[22] of several solvents. For molecular solvents, each window with a width of pK_S is arranged by placing their left-end at −log $\gamma_{t,H}$: the transfer activity coefficient of H^+ from water to the solvent.[53] Therefore, these windows lie on the universal pH-scale or, in other words, solutions of identical pH in this scale have an identical H^+ activity. By using this diagram, we can easily compare the acidity and basicity of solutions beyond the solvents. Here, we attempt to arrange the pH-windows of the present PILs. However, $\gamma_{t,H}$ from water to the respective PIL is not available at the present stage. Though rough, the pHwindows are arranged according

to the basicity because the conjugate base of the present PILs is C_1Im in common. Thus, pH-windows of the PILs are arranged by placing their right-end at pH = pK_a(C_1hIm$^+$). We, of course, recognize that it is quite a rough estimation because $\gamma_{t,C1Im}$, as well as the temperature dependence in pK_S, are not taken into account. Nonetheless, we emphasize Figure 5 is practically useful. With regard to C_1hIm$^+$$Tf_2N^-$ and C_1hIm$^+$$TfO^-$, the negative leftmost values and much smaller rightmost values than 14 indicate these PILs are possibly classified into acidic solvents. It should be emphasized that the gap in the leftmost values (0.35) is significantly smaller than that in the gas phase acidity of Tf_2NH and TfOH; that for Tf_2NH is about 55 kJ/mol smaller, which corresponds to more acidic of 10 in pH unit at 298 K, than that for TfOH.[19,20] This suppression arises from a large salvation free energy of the species, HA and A^-, as well as C_1Im and C_1hIm$^+$ in PIL. Watanabe et al. proposed a parameter ionicity as a measure of the ion−ion interaction in RTILs.[54,55] Watanabe's ionicity is larger in C_4mim$^+$$Tf_2N^-$ (C_4mim$^+$: 1-buthyl-3-methylimidazolium) than that in C_4mim$^+$$TfO^-$, indicating that C_4mim$^+$ is more strongly interacting with TfO^- than Tf_2N^- in these RTILs. Therefore, C_1hIm$^+$ should be stabilized extensively in C_1hIm$^+$$TfO^-$ than in C_1hIm$^+$$Tf_2N^-$. This may lead to increasing pK_S in C_1hIm$^+$$TfO^-$. The salvation effect on HA also varies its acidity, while it cannot be separated from that on C_1Im. Thus, the ion−ion interaction and the solvation of ions in PILs play a key role in the acidity and basicity of PILs as solvents. In the case of C_1hIm$^+$$CF_3COO^-$, the pH-window lies completely inside that of water. In Figure 6, directly obtained autoprotolysis constant pK_S is plotted against ΔpK_a, together with those for EAN[27] and a series of PILs composed of ammonium with a 2-hydroxyethyl group(s) as a cation.[56] We employed −4 for pK_a of Tf_2NH in water to calculate ΔpKa, as heretofore used.[3,23,33] As shown, pK_S of PILs have a good correlation with ΔpK_a; plots for C_1hIm$^+$$Tf_2N^-$, C_1hIm$^+$$CF_3COOH$, C_1Im−CH_3COOH, and C_1Im−HCOOH, as well as EAN, almost fall on a straight line with a slope of unity. Furthermore, data for the PILs consisting of a cation with a 2-hydroxyethyl group(s) also practically

fall on the same line. On the other hand, plots for $C_1hIm^+TfO^-$ were rather scattered, depending on the employed values of pK_a for TfOH in an aqueous solution. If we here adopt pK_a = −4.5 for TfOH in the aqueous solution, the plot locates near the above-mentioned straight line. Figure 6 possibly implies that the acid−base property of PILs can be approximately predicted from pK_as of the constituent ions in an aqueous phase. However, it would not always be true. Further investigations such as thermodynamics of acid-dissociation of solutes in PILs are required and are now going on.

3-4. CONCLUSION

Proton-donating and ionization properties of several protic ionic liquids (PILs) made from C_1Im and a series of acids have been assessed by means of potentiometric and calorimetric titrations. With regard to strong acids, Tf_2NH and TfOH, it was elucidated that the two equimolar mixtures with C_1Im almost consist of ionic species, C_1hIm^+ and A^-, and the proton transfer equilibrium corresponding to autoprotolysis in ordinary molecular liquids was established. The respective autoprotolysis constants were successfully evaluated, which indicate the proton-donating abilities of TfOH and Tf_2NH in the respective PILs are similar. In the case of trifluoroacetic acid, the proton-donating ability of CF_3COOH is much weaker than those of TfOH and Tf_2NH, while ions are predominant species. On the other hand, with regard to formic acid and acetic acid, protons of these acids are suggested not to transfer to C_1Im sufficiently. From calorimetric titrations, about half of C_1Im is estimated to be protonattached at most in the CH_3COOH−C_1Im equimolar mixture. In such a mixture, hydrogen-bonding adducts formation has been suggested. The autoprotolysis constants of the present PILs show a good linear correlation with dissociation constants of the constituent acids in an aqueous phase.

3-5. REFERENCES

1. Gabriel, S.; Weiner. J. Ber. Dtsch, *Chem. Ges.* **1888**, *21*, 2664−2669.
2. Walden, P. Bull. *Acad. Imp. Sci. (St. Petersburg)* **1914**, *8*, 405.

3. MacFarlane, D. R.; Pringle, J. M.; Johansson, K. M.; Forsyth, S. A.; Forsyth, M. *Chem. Commun.* **2006**, 1905−1917.
4. Greaves, T. L.; Weerawardena, A.; Fong, C.; Krodkiewska, I.;Drummond, C. J. *J. Phys. Chem. B* **2006**, *110*, 22479−22487.
5. Hirao, M; Sugimoto, H; Ohno, H *J. Electrochem. Soc.* **2000**, *147*,4168−4172.
6. Ohno, H; Yoshizawa, M *Solid State Ionics* **2002**, 154−155, 303−309.
7. Johnson, K. E.; Pagni, R. M.; Bartmess, *J. Monatsh. Chem.* **2007**, *138*, 1077−1101.
8. Greaves, T. L.; Drummond, C. *J. Chem. Rev.* **2008**, *108*, 206−237.
9. Hajipour, A. R.; Rafiee, F. *Org. Prep. Proc. Int.* **2010**, *42*, 285−362.
10. MacFarlane, D. R.; Vijayaraghavan, R.; Ha, H. N.; Izgorodina, A.; Weaver, K. D.; Elliott, G. D. *Chem. Commun.* **2010**, *46*, 7703−7705.
11. Xu, W.; Angell, C. A. *Science* **2003**, *302*, 422−425.
12. Susan, M. B. H.; Noda, A.; Mitsushima, S.; Watanabe, M. *Chem. Commun.* **2003**, 938−939.
13. Noda, A.; Susan, M. A. B. H.; Kudo, K.; Mitsushima, S.; Hayamizu, K.; Watanabe, M. *J. Phys. Chem. B* **2003**, *107*, 4024−4033.
14. Belieres, J-.P.; Gervasio, D.; Angell, C. A. *Chem. Commun.* **2006**, 4799−4871.
15. Nakamoto, H.; Noda, A.; Hayamizu, K.; Hayashi, S.; Hamaguchi, H.; Watanabe, M. *J. Phys. Chem. C* **2007**, *111*, 1541−1548.
16. Stoimenovski, J; Izgorodina, E. I.; MacFarlane, D. R. *Phys. Chem. Chem. Phys.* **2010**, *12*, 10341−10347.
17. Thomazeau, C; Olivier-Bourbigou, H.; Magna, L.; Luts, S.; Gilbert, B. *J. Am. Chem. Soc.* **2003**, *125*, 5264−5265.
18. Robert, T.; Magna, L.; Olivier-Bourbigou, H.; Gilbert, B. *J.Electrochem. Soc.* **2009**, *156*, F115−F121.
19. Koppel, I. A.; Taft, R. W.; Anvia, F.; Zhu, S.-Z.; Hu, L.-Q.; Sung, K.-S.; DesMarteau, D. D.; Yagupolskii, L. M.; Yagupolskii, Y. L.; Vlasov, V. M.; Notario, R.; Maria, P.-C. *J. Am. Chem. Soc.* **1994**, *116*, 3047−3057.
20. Leito, I.; Raamat, E.; Kutt, A.; Saame, J.; Kipper, K.; Koppel, I. A.; Koppel, I.; Zhang, M.; Mishima, M.; Yagupolskii, L. M.; Garlyauskayte, R. Y.; Filatov, A. A. *J. Phys. Chem. A* **2009**, *113*, 8421−8424.
21. Barhdadi, R.; Troupel, M.; Comminges, C.; Laurent, M.; Doherty, A. *J. Phys. Chem.*

B **2012**, *116*, 277−282.

22. Izutsu, K Electrochemistry in Nonaqueous Solutions, *2nd ed.; Wiley-VCH: New York*, **2009**; Chapter 3.
23. Yoshizawa, M.; Xu, W.; Angell, C. A. *J. Am. Chem. Soc.* **2003**,*125*, 15411−15419.
24. Belieres, J.-P.; Angell, C. A. *J. Phys. Chem. B* **2007**, *111*, 4926−4937.
25. Angell, C. A.; Byrne, N.; Belieres, J.-P. *Acc. Chem. Res.* **2007**, *40*,1228−1236.
26. Bautista-Martinez, J. A.; Tang, L.; Belieres, J.-P.; Zeller, R.; Angell, C. A.; Friesen, C. *J. Phys. Chem. C* **2009**, *113*, 12586−12593.
27. Kanzaki, R; Uchida, K.; Hara, S.; Umebayashi, Y.; Ishiguro, S.; Nomura, S. *Chem. Lett.* **2007**, *36*, 684−685.
28. Kanzaki, R.; Uchida, K.; Song, X.; Umebayashi, Y.; Ishiguro, *S. Anal. Sci.* **2008**, *24*, 1347−1349.
29. Kanzaki, R.; Song, X.; Umebayashi, Y.; Ishiguro, S. *Chem. Lett.***2010**, *39*, 578−579.
30. Kakiuchi, T. J. *Solid State Electrochem.* **2011**, *15*, 1661−1671. Sakaida, H.; Kakiuchi, T. *J. Phys. Chem. B* **2011**, *115*, 13222−13226. Kakiuchi, T.; Yoshimatsu, T.; Nishi, N. *Anal. Chem.* **2007**, *79*, 7187−7191.
31. Olah, G. A.; ; Prakash, G. K. S.; Sommer, J. Superacids; John *Wiley & Sons: New York*, **1985**.
32. Olah, G. A. *J. Org. Chem.* **2005**, *80*, 2413−2429.
33. Mihichuk, L. M.; Driver, G. W.; Johnson, K. E. *Chem. Phys. Chem.* **2011**, *12*, 1622−1632.
34. Howells, R. D.; McCown, J. D. *Chem. Rev.* **1977**, *77*, 69−92.
35. Yeston, J. S. *Science* **2004**, *306*, 781. Stoyanov, E. S.; Kim, K.-C.; Reed, C. A. *J. Phys. Chem. A* **2004**, *108*, 9310−9315.
36. Foropoulos, J., Jr.; DesMarteau, D. D. *Inorg. Chem.* **1984**, *23*, 3720−3723.
37. Tolstoy, P. M.; Guo, J.; Koeppe, B.; Golubev, N. S.; Denisov, G. S.; Smirnov, S. N.; Limbach, H.-H. *J. Phys. Chem. A* **2010**, *114*, 10775−10782.
38. Schuster, I. I.; Roberts, J. D. *J. Org. Chem.* **1979**, *44*, 3864−3867.
39. Berg, R. W.; Lopes, J. N. C.; Ferreira, R; Rebelo, L. P. N.;Seddon, K. R.; Tomaszowska, A. A. *J. Phys. Chem. A* **2010**, *114*, 10834−10841.
40. Gomez, P. C.; Pacios, L. F. *Phys. Chem. Chem. Phys.* **2005**, *7*, 1374−1381.
41. See, for example: Yasaka, Y.; Yoshida, K.; Wakai, C.; Matubayasi, N.; Nakahara,

M. *J. Phys. Chem. A* **2006**, *110*, 11082.

42. (a) Christensen, J. J.; Hanse, L. D.; Izatt, R. M. Handbook of Proton Ionization Heats; *Wiley: New York*, **1976**, (b) Morel, J.-P.; Fauve, J.; Avedikian, L.; Juillard, J. *J. Solution Chem.* **1974**, *3*, 403.
43. Konicek, J.; Wadso, I. *Acta Chem. Scand.* **1970**, *24*, 2612−2616.
44. Eyet, N.; Villano, S. M.; Bierbaum, V. M. *Int. J. Mass Spectrom.* **2009**, *283*, 26−29.
45. Nakabayashi, T.; Kosugi, K.; Nishi, N. *J. Phys. Chem. A* **1999**, *103*, 8595−8603.
46. Taylor, M. D. *J. Am. Chem. Soc.* **1951**, *73*, 315−317.
47. Frurip, D. J.; Curtiss, L. A.; Blander, M. *J. Am. Chem. Soc.* **1980**, *102*, 2610−2616.
48. Gaufres, R.; Norbygaard, T. *Appl. Spectrosc. Rev.* **2006**, *41*, 165−183.
49. Domanska, U.; Marciniak, A. *Fluid Phase Equilib.* **2005**, *238*, 137−141.
50. Bustamante, P.; Drago, R. S. *J. Phys. Chem. B* **1997**, *101*, 5002−5009.
51. Orzechowski, K.; Pajdowska, M.; Czarnecki, M.; Kaatze, U. *J.Mol. Liq.* **2007**, *133*, 11−16.
52. Johansson, K. M.; Izgorodina, E. I.; Forsyth, M.; MacFarlane, D. R.; Seddon, K. R. *Phys. Chem. Chem. Phys.* **2008**, 2972−2978.
53. Marcus, Y *Pure Appl. Chem.* **1983**, 977−1021.
54. Tokuda, H.; Hayamizu, K.; Ishii, K.; Susan, M. A. B. H.; Watanabe, M. *J. Phys. Chem. B* **2004**, *108*, 16593−16600.
55. Tokuda, H.; Tsuzuki, S.; Susan, M. A. B. H.; Hayamizu, K.; Yatanabe, M. *J. Phys. Chem. B* **2006**, *110*, 19593−19600.
56. Song, S.; Kanzaki, R.; Ishiguro, S.; Umebayashi, Y. *Anal. Sci.* **2012**, *28*, 469−474.

Chapter 3

Figures and Tables

Acid−Base Property of *N*-Methylimidazolium-Based Protic Ionic Liquids Depending on Anion

Table 1. Obtained pK_S and $E°$'

acid	T / K	density/g cm^{-3}	pK_a(HA) [a]	pK_{PIL}	$E°$ / mV
Tf_2NH	325	1.5948		8.58 (0.10)	372 (5)
TfOH	367	1.3376		8.93 (0.09)	153 (5)
CF_3COOH	338	1.3445	0.5	3.14 (0.07)	-361 (3)
HCOOH	298	1.1322	3.764	−1.4 [b]	
CH_3COOH	298	1.0712	4.756	−1.4 [b]	

[a] Acid dissociation constant in aqueous phase, [b] estimated at equimolar mixture by calorimetric titration (see text). the numbers in parentheses refer to three standard deviations.

Figure 1

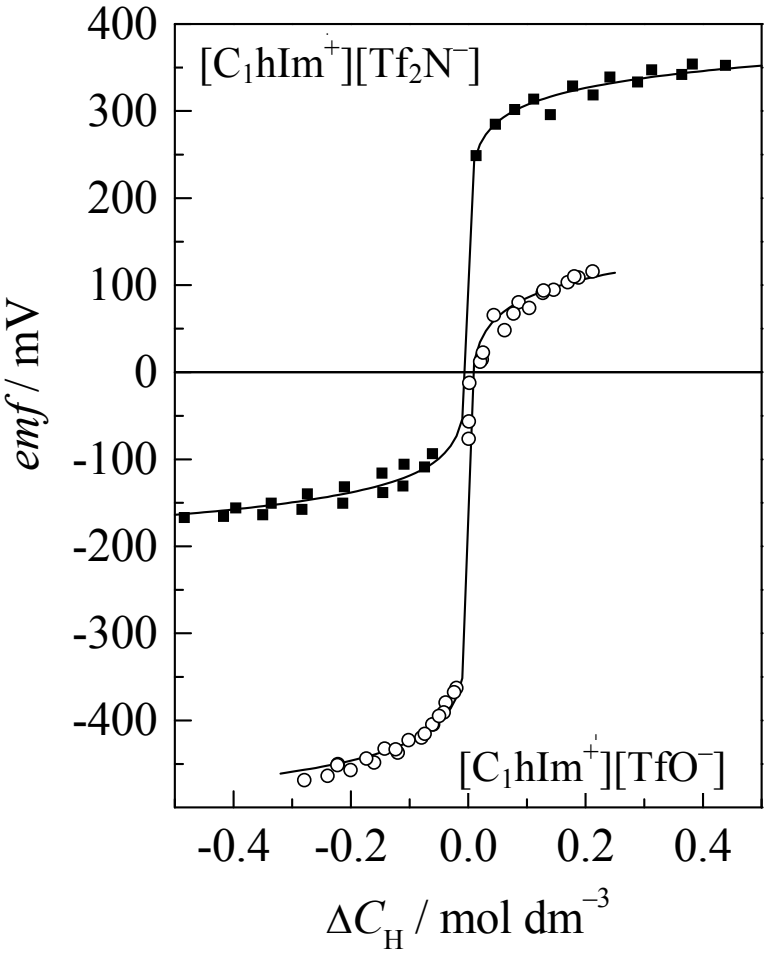

Figure 1. Potentiometric titration curves in $C_1hIm^+Tf2N^-$ (closed squares) and $C_1hIm^+TfO^-$ (opened circles).

Figure 2

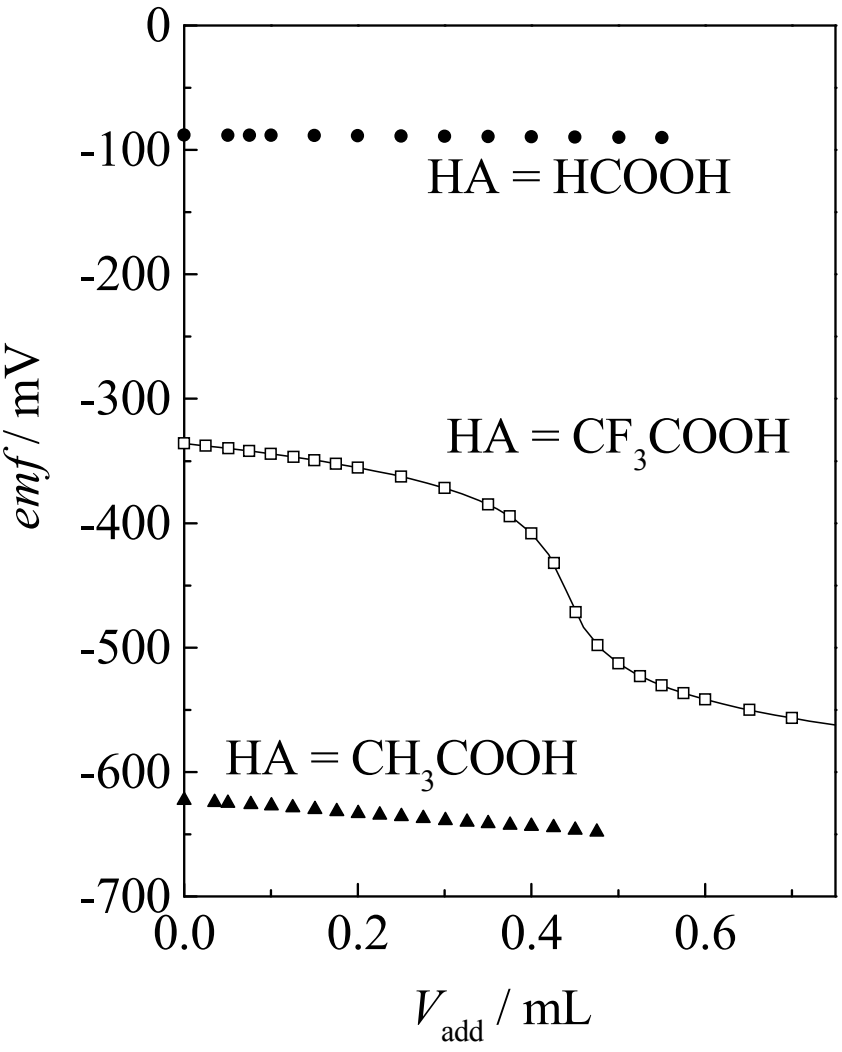

Figure 2. Potentiometric titration curves in $C_1hIm^+CF_3COO^-$ (opened squares) and the mixtures of $CH_3COOH-C_1Im$ (closed triangles) and $HCOOH-C_1Im$ (closed circles). The solid lines are guides to the eye.

Figure 3

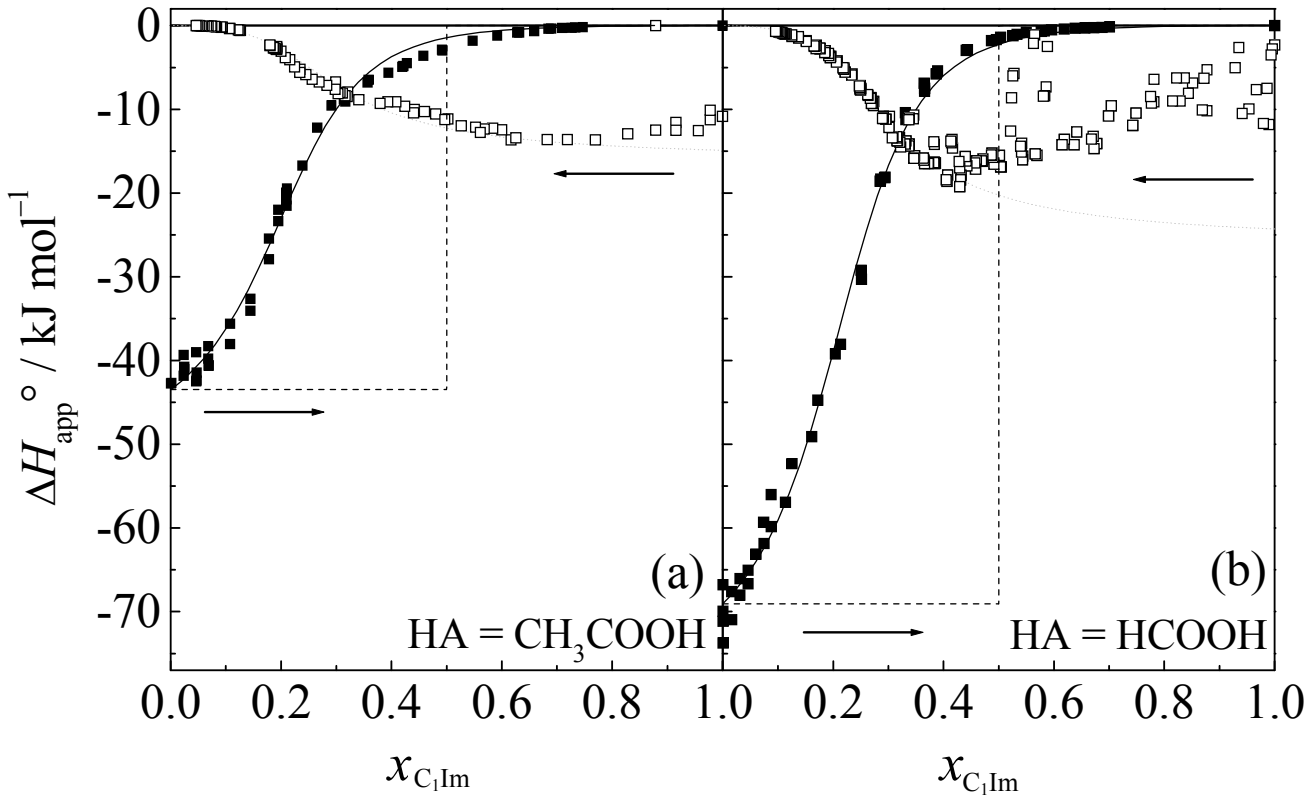

Figure 3. Calorimetric titration curves in (a) $CH_3COOH-C_1Im$ and (b)$HCOOH-C_1Im$ mixtures in apparent reaction enthalpy ΔH_{app}°. The closed and opened symbols denote the titration by C_1Im and HA, respectively. The arrows indicate the direction of the titration.

Figure 4

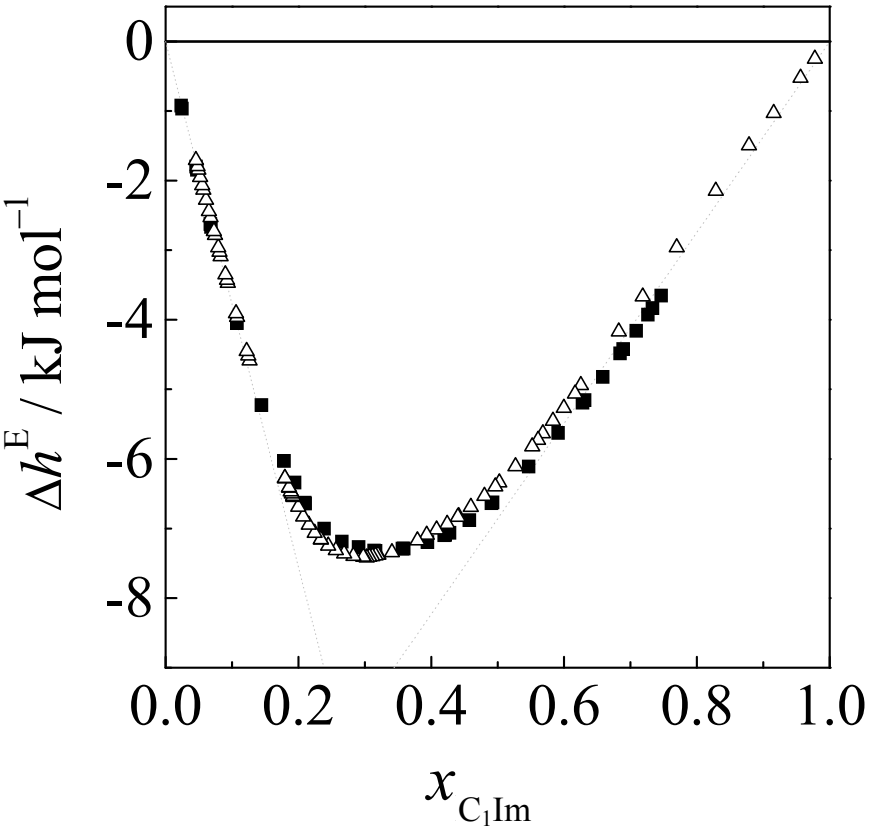

Figure 4. Excess enthalpy of mixing of CH_3COOH and C_1Im. The closed and opened symbols denote the titration by C_1Im and CH_3COOH, respectively.

Figure 5

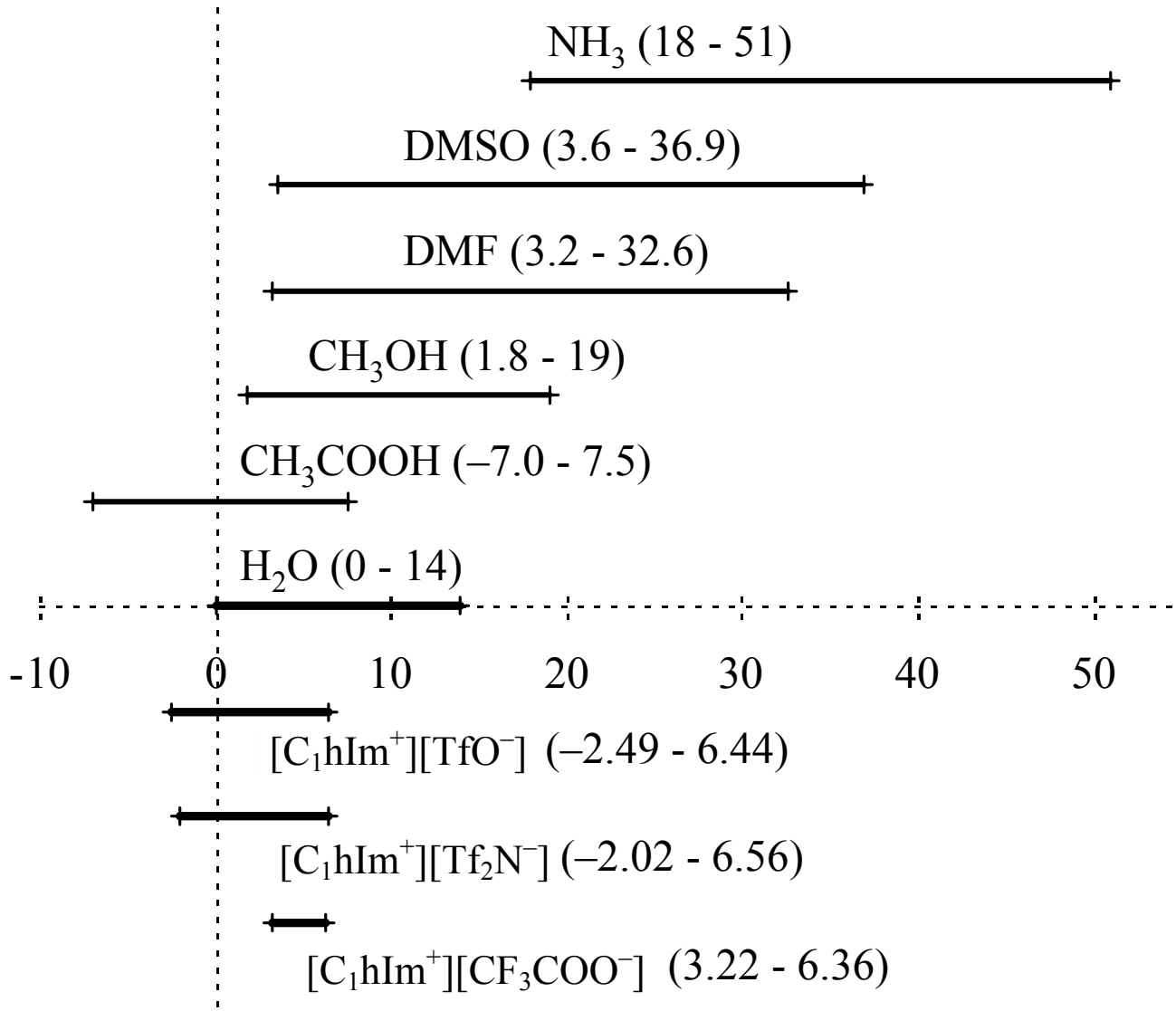

Figure 5. pH-windows in various solvents, including PILs, shown by a common pH scale[22] (DMF = *N*,*N*-dimethylformamide, DMSO = *N*,*N*dimethylsulfoxide).

Figure 6

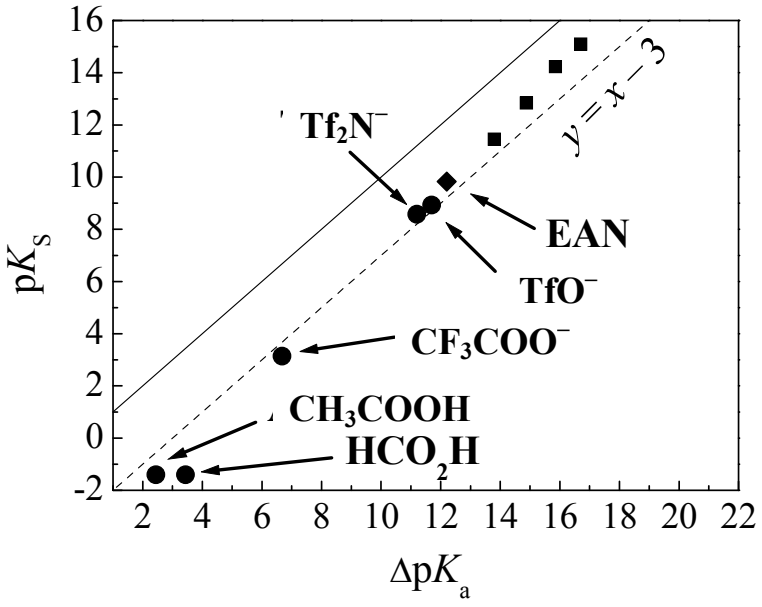

Figure 6. Relationship between ΔpK_a and pK_S in the present PILs. The closed diamonds are for EAN[27] and a series of PILs composed of a ternary ammonium with 2-hydroxyethyl group(s).[56]

Chapter 4

A Novel Proton Conductive Liquid with No Ions: *Pseudo* Protic Ionic Liquids

4-1. INTRODUCTION

Room-temperature ionic liquids have attracted remarkable attention as new materials for various chemical applications.[1] Ionic liquids can be classified into two categories of protic and aprotic ones in terms of dissociable hydrogen atom(s).[2] Modern protic ionic liquids $[HB^+][A^-]$ have been reported for the first time by Ohno and co-workers,[3] in which HB^+ and A^- stand for the conjugated cation and anion of a Brønsted base B and acid HA, respectively. It is proposed that protic ionic liquids can be utilized as protonconductive materials toward a new class of fuel cells.[4–6] Since then, various protic ionic liquids have been proposed. Toward a new class of nonhumidified intermediate temperature fuel cells by using protic ionic liquids, Angell and coworkers demonstrated that ΔpK_a can be a good measure.[5] ΔpK_a is defined as $\Delta pK_a = pK_a(HB^+) - pK_a(HA)$, in which $pK_a(HB^+)$ and $pK_a(HA)$ represent negative value of common logarithms of the acid dissociation constant for HB^+ and HA, respectively, in each aqueous solution. According to Angell and co-workers,[5] the protic ionic liquids of a ΔpK_a value greater than 10 can be classified as "good ionic liquids", because they should have a relatively high boiling point to exhibit practically similar ion conductive behavior with aprotic ones in terms of the Walden rules. On the other hand, those of small ΔpK_a are "poor ionic liquids", because proton transfer from HA to B may be incomplete in this subclass of protic ionic liquids to give a low boiling point and less ionic conductivity. Hence, the experimental effort has been made to directly evaluate values corresponding to the ΔpK_a in neat ionic liquids.[7] However, as can be easily noticed from the definition, the ΔpK_a corresponds to the proton-transfer equilibrium $HB^+ + A^- \leftrightarrow B + HA$ in an aqueous solution, not that in ionic liquids. Therefore, ΔpK_a is qualitative, though it is practically useful.[8] As was established in the last several

decades,[9] hydration plays a crucial role in an acid/base property of the solute in aqueous solutions, so that it is needed to directly assess an acid/base property of ionic liquids as the solvent to reveal reliable acidity or basicity of ionic liquids quantitatively. We reported autoprotolysis constants K_S for the representative ionic liquid ethylammonium nitrate and its aqueous mixtures by direct potentiometry and calorimetry.[10] It should be noted that K_S for the reaction $HB^+ + A^- \leftrightarrow B + HA$ in the ionic liquid was directly evaluated, so that pK_S is essentially different from ΔpK_a due to solvation of both reactants and products. Recently, we extended our work to various *N*-methylimidazolium (C_1hIm^+)-based protic ionic liquids and found that no significant jump was observed in the electromotive force at the respective equivalence point for the mixtures of formic acid or acetic acid (AcOH) with *N*-methylimidazole (C_1Im); probably, these pK_S values are negative.[11] This experimental evidence suggests that the proton of acetic acid hardly transfers to C_1Im to give a nonaqueous solvent mixture rather than a protic ionic liquid. Interestingly, considerable ionic conductivity had been reported for the C_1Im and AcOH equimolar mixture.[2a)] Herein, for further insight into ion-conductive behavior of the C_1Im and AcOH equimolar mixture, Raman spectroscopic study with the aid of quantum calculations was performed, and ionic conductivity, viscosity, and density were measured at various temperatures.

4-2. EXPERIMENTAL

4-2-1. Materials

C_1Im and AcOH were dried over a molecular sieve 4Å for several weeks, and then each was distilled under reduced and ambient pressure, respectively. Equivalent amount of each liquid was mixed with a gradual droplet addition of the acid to the base avoiding vaporization by generation of the heat of mixing. Purity and a water content of the final equimolar mixture were checked by elemental analysis and the Karl-Fischer titration,

respectively. All chemicals were treated and stored in a glove box, in which a water content was kept less than 1 ppm.

4-2-2. Raman spectroscopic Measurements

FT-Raman spectrometer Perkin-Elmer GX-R was used. Details of the Raman measurement were similar to those described in elsewhere. [21]

4-2-3. Ionic conductivity, viscosity and density

Ionic conductivity was measured with ALS/H Instruments model 604C electrochemical analyzer. Viscosity was measured with Lauda iVisc and Brookfield DV-II+ Pro viscometers calibrated with glycol aqueous solutions at various temperatures. Density was measured with a KEK DA-310 vibration tube density-meter after calibration with dried air and degassed water at each temperature. All measurements were carried out within temperature fluctuation of ±0.1 K at a given temperature.

4-2-4. Molecular orbital calculations

Quantum calculations were carried out for an isolated molecules, ions and ion pairs (finally molecular complexes) in gas phase at the B3LYP/6-311+G(d,p) level of theory. Basis set superposition error (BSSE) was corrected by a counterpoise method. Polarizable continuum model (PCM) was used for the calculations in acetonitrile. In the PCM calculations, atomic radii including a hydrogen atom were explicitly considered by using those in the UFF force fields. For the species in dielectric solutions, the BSSE correction was also estimated with single point calculations in gas phase at the optimized geometry in solutions. Normal vibration analysis was performed for all of the species at the optimized geometries except scanning potential energy surfaces to confirm they have no imaginary frequency. *Gaussian03* program suite was used for all quantum chemical calculations. [22]

4-3. RESULT AND DISCUSSION

At first, Raman spectrum of C_1Im and AcOH equimolar mixture was recorded in the frequency range of ν= 200 – 1800 cm^{-1} at an ambient temperature, and data are in good agreement with that previously reported by Berg et al.[12] Figure 1 shows representative Raman bands accompanied by ν(CC) and ν(CO) stretching vibrations of $AcOH/AcO^-$,[13] and $\nu_{ring}+\delta(CH_3)+\nu(N\text{-}CH_3)$ and $\nu_{ring}+\delta(CH_3)$ of C_1Im/C_1hIm^+.[14] Clearly, when acetic acid dissociates, ν(CC) and ν(CO) bands shift toward higher and lower frequency, respectively. Similarly, two bands of $\nu_{ring}+\delta(CH_3)+\nu(N{-}CH_3)$ and $\nu_{ring}+\delta(CH_3)$ originating from C_1Im shift toward higher frequency when it protonates. However, the possibly corresponding Raman bands for the mixture were appeared at ν=884 and 1710 cm^{-1} for $AcOH/AcO^-$ and at 1520 cm^{-1} with two shoulders of 1509 and 1530 cm^{-1} for C_1Im/C_1hIm^+, respectively, which suggests that electrically neutral molecules AcOH and C_1Im predominantly exist in the mixture. Peak positions of other Raman bands for the mixture gave better linear relationships with those for the respective neat liquid relative to those for $[C_1hIm^+]$ $[Cl^-]$ and 1 $moldm^{-3}$ NaOAc aqueous solution (Figure 6a). In addition, any Raman bands ascribable to the ions C_1hIm^+ and AcO^- could not be found in the Raman spectrum for the mixture. Hence, we concluded that the proton of the AcOH hardly transfers to the C_1Im in the mixture. This Raman spectroscopic evidence strongly supports our previous thermodynamic results on the autoprotolysis equilibrium in the mixture.[11] For further insight, quantum calculations were performed. First, the optimized geometries of C_1hIm^+ and AcO^- were obtained in the respective isolated gas phase. Then, geometry optimizations of hydrogen-bonded ion pair of $C_1hIm^+\cdots AcO^-$ were carried out, but failed. As was expected due to stronger electrostatic interaction between proton and AcO^-, the proton of C_1hIm^+ moved to the AcO^- carbonyl oxygen during geometry optimization to give molecular complex $C_1Im\cdots AcOH$ with two hydrogen bonds of the $OH\cdots N$ and the $C_2H\cdots O$ (molecular complex 1, see Figure 7). The molecular complex 1 is in good accordance with that previously found by

Berg et al.[12] Similar doubly hydrogen-bonded molecular complex 2 with slightly higher energy was obtained as the optimized geometry, in which there are the OH···N and the C_4H···O hydrogen bonds. Potential-energy surface (PES) of this kind of proton strongly depends on the surroundings;[15] actually, it is known that AcOH of pK_a 4.7 act as a stronger acid than C_1hIm^+ of pK_a 7.1 in the respective aqueous solution. In acetonitrile with the PCM calculations, the ion pairs 1 and 2 corresponding to the molecular complexes 1 and 2, respectively, were successfully optimized with higher energy of about 7 $kJmol^{-1}$ relative to the molecular complexes. The energy difference of 7 $kJmol^{-1}$ corresponds to concentration ratio of 0.06 for the ion pairs against the molecular complexes, which agrees well with our Raman spectroscopic and thermodynamic results (Figure 2).

We also attempted to assign experimental Raman spectrum of the mixture on the basis of theoretical ones. Please note that it has been proposed that the cyclic and/or the chainlike hydrogen-bonded species exist in neat AcOH.[16] Thus, we calculated theoretical Raman bands for the cyclic dimer and the chain oligomers $(AcOH)_n$ of n=2–4, and the cyclic dimer gave the most satisfactory result. The observed Raman shifts were plotted against those theoretically calculated for the isolated C_1Im and AcOH cyclic dimer. The plots gave nearly straight line. The linear slope and intercept were closer to unity and zero than those evaluated for the isolated C_1hIm^+ and AcO^-, suggesting that the observed Raman spectrum for the mixture can be adequately attributable to sum of those arising from electrically neutral species of C_1Im and AcOH. Moreover, theoretical Raman spectra of the molecular complexes and the ion pairs obtained with the PCM calculations were also tested. The former can explain the experimental Raman spectrum more satisfactorily than the latter (these results are shown in Figure 6b and c). Hence, we finally concluded that neutral molecular species of C_1Im and AcOH predominantly (or much excess) exist in their mixture. As was mentioned above, though the ΔpK_a value for this system is 2.4, which means C_1Im and AcOH are produced

only 1/250 relative to C_1hIm^+ and AcO^- in the aqueous solution, electrically neutral molecular species of C_1Im and AcOH mainly exist in the mixtures. Nevertheless, significantly large ionic conductivity of 4 $mScm^{-1}$ has been reported for the C_1Im and AcOH equimolar mixture at an ambient temperature.[2a] This is quite surprising, although ionic species are actually rather minor in the mixture. Therefore, ionic conductivity, viscosity, and density were measured at various temperatures to clarify the ion conductive behavior of the mixture. Ionic conductivity of 5.9 $mScm^{-1}$ and viscosity of 6.6 MPa s at an ambient temperature are in good agreement with those reported by MacFarlane et al.[2a] The respective temperature dependence and the Vogel–Fulcher–Tummann (VFT) least squares fittings for ionic conductivity and viscosity and a linear one for density are depicted in Figure 8, indicating that all of parameters were evaluated adequately. Though Watanabe and co-workers have proposed the ionisity based on the ionic conductivity with the AC impedance and that estimated from the Nernst–Einstein equation with the pulsed gradient spin-echo (PGSE) NMR self-diffusion coefficient,[17] the Walden plots are also useful for discussion on the ion-conductive behavior. Figure 3 shows the Walden plots for the C_1Im and AcOH equimolar mixture. It should be noted that no significant Raman bands arising from the ionic species were found in Raman spectra of the mixture. This indicates that the ionic species may exit at most below 1:100 relative to the respective neutral component. The molar ionic conductivity for the mixture was thus estimated based on the Raman observation. As can be clearly seen from Figure 3, in which data for 4 $moldm^{-3}$ sulfuric acid and for 98% phosphoric acid are also plotted for comparison, the plots for the C_1Im and AcOH equimolar mixture locate above the ideal Walden line, and are close to those for the aqueous acid solutions. This suggests that the C1Im and AcOH equimolar mixture has specific ion-conductive mechanism, such as the Grötthuss one in aqueous solutions; in this context, it could be a good or *superionic* liquid according to the Angell's classification. Although PES of the proton in the mixture was not clear at the present stage (i.e., whether single minimum or double

minima), it was worth discussing the proton-conductive mechanism in the mixture on the basis of aforementioned quantum calculations. According to the Bell–Evans–Polanyi principle,[18] activation energy for the proton transfer from the carbonyl oxygen to the imidazole nitrogen might be small of a few kJmol^{-1} in the mixture because of the small (free) energy difference of approximately 7 kJmol^{-1} between the molecular complexes and the ion pairs. Such small activation energy could be comparable with the thermal energy of kT at an ambient temperature, suggesting fast proton transfer. When the ionic species are produced in the mixture, the surrounding molecules should be reoriented or rotate as suitable for the ions solvation. This might be fast, because the surrounding molecules are electrically neutral. Fast proton transfer and reorientation of the surroundings might lead to specific proton conduction, such as a proton relay mechanism. A possible, though speculative, protonconduction mechanism would be shown in Figure 4. Moreover, networked liquid structure with hydrogen bonds may play a crucial role in specific proton conduction.[19] For the networked hydrogen-bonding liquid structure, the dielectric relaxation experiment was useful.[20] The C_1Im and AcOH equimolar mixture showed relatively large permittivity from preliminary measurements by our collaborators, which suggests there is hydrogen-bonded network structure in the mixture. More investigation by means of self-diffusion coefficient with the PGSE NMR and/or neutron/X-ray scattering experiments is needed for detailed discussion on the protonconduction mechanism and/or liquid structure, and are now ongoing in our group.

4-4. CONCLUSION

Since Arrhenius theory of electrolytic dissociation, it has been believed that salt dissociates in solution to contribute to electric conduction. However, we found that two equimolar insulator nonaqueous solvents of N-methylimidazole (($pK_S = \sim 20$) and acetic acid ($pK_S = -14$) could give the

liquid with hydrogen-bonded network structure to show proton conductive behavior, although the mixture is practically composed of just electrically neutral molecular species, not ions. Hence, it may be suitable to call such liquids "*pseudo*-ionic liquids" rather than "ionic liquids".

4-5. REFERENCES

1. M. Armand, F. Endres, D. R. MacFarlane, H. Ohno, B. Scrosati, *Nature Materials* **2009**, *8*, 621-629.
2. a) D. R. MacFarlane, J. M. Pringle, K. M. Johansson, S. A. Forsyth, M. Forsyth, *Chem*. *Commun*. **2006**, 1905-1917. b) T. L. Greaves, C. J. Drummond, *Chem*. *Rev*. **2008**, *108*, 206-237. c) L. M. Mihichuk, G. W. Driver, K. E. Johnson, *ChemPhysChem* **2011**, *12*, 1622-1632.
3. a) M. Hirao, H. Sugimoto, H. Ohno, *J*. *Electrochem*. *Soc*. **2000**, *147*, 4168-4172. b) M. Yoshizawa, W. Ogihara, H. Ohno, *Electrochem*. *Solid-State Lett*. **2001**, *4*, E25-E27. c) H. Ohno, M. Yoshizawa, *Solid State Ionics* **2002**, *154-155*, 303-309.
4. a) Md. A. B. H. Susan, A. Noda, S. Mitsushima, M. Watanabe, *Chem*. *Commun*. **2003**, 938-939. b) A. Noda, Md. A. B. H. Susan,; K. Kudo, S. Mitsushima, K. Hayamizu, M. Watanabe, *J*. *Phys*. *Chem*. *B* **2003**, *107*, 4024-4033.
5. a) M. Yoshizawa, W. Xu, C. A. Angell, *J*. *Am*. *Chem*. *Soc* **2003**, *125*, 15411-15419. b) W. Xu, C. A. Angell, *Science* **2003**, *302*, 422-425. c) J-P. Belieres, C. A. Angell, *J*. *Phys*. *Chem*. *B* **2007**, *111*, 4926-4937.
6. U. A. Rana, M. Forsyth, D. R. MacFarlane, J. M. Pringle, *Electrochim*. *Acta* **2012**, *84*, 213-222.
7. J.A. Bautista-Martinez, L. Tang, J-P. Belieres, R. Zeller, C. A. Angell, C. Friesen, *J*. *Phys*. *Chem*. *C* **2009**, *113*, 12586-12593.
8. a) M. S. Miran, H. Kinoshita, T. Yasuda, Md. A. B. H. Susan, M. Watanabe, *Chem*. *Commun*. **2011**, *47*, 12676-12678. b) M. S. Miran, H. Kinoshita, T. Yasuda, Md. A. B. H. Susan, M. Watanabe, *Phys*. *Chem*. *Chem*. *Phys*. **2012**, *14*, 5178-5186. c) M. S. Miran, T. Yasuda, Md. A. B. H. Susan, K. Dokko, M. Watanabe, *RSC Advances* **2013**, *3*,

4141-4144.

9. a) P. Love, R. B. Cohen, R. W. Taft, *J. Am. Chem. Soc.* **1968**, *90*, 2455-2462. b) M. J. Locke, M. J.; R. T. McIver, Jr. *J. Am. Chem. Soc.* **1983**, *105*, 4226-4232. c) R. S. Drago, T. R. Cundari, D. C. Ferris, *J. Org. Chem.* **1989**, *54*, 1042-1047.
10. a) R. Kanzaki, K. Uchida, S. Hara, Y. Umebayashi, S. Ishiguro, S. Nomura, *Chem. Lett.* **2007**, *36*, 684-685. b) R. Kanzaki, K. Uchida, X. Song, Y. Umebayashi, S. Ishiguro, *Anal. Sci.* **2008**, *24*, 1347-1349. c) R. Kanzaki, X. Song, Y. Umebayashi, S. Ishiguro, *Chem. Lett.* **2010**, *39*, 578-579. d) X. Song, R. Kanzaki, S. Ishiguro, Y. Umebayashi, *Anal. Sci.*, **2012**, *28*, 469-474.
11. R. Kanzaki, H. Doi, X. Song, S. Hara, S. Ishiguro, Y. Umebayashi, *J. Phys. Chem. B* **2012**, *116*, 14146-14152.
12. R. W. Berg, J. N. C. Lopes, R. Ferreira, L. P. N. Rebelo, K. R. Seddon, A. A. J. Tomaszowska, *J. Phys. Chem. A* **2010**, *114*, 10834-10841.
13. F. Quiles, A. Burneau, *Vib. Spectrosc.* **1998**, *16*, 105–117.
14. a) G. Perchard, A. Novak, *Spectrochim Acta*, *Part A*, **1967**, *23* 1953. b) R. L. Dean, J. L. Wood, *J. Mol. Structure*, **1975**, *26*, 197-213.
15. P. C. Gómez, L. F. Pacios, *Phys. Chem. Chem. Phys.* **2005**, *7*, 1374-1381.
16. a) K. Kosugi, T. Nakabayashi, N. Nishi, *Chem. Phys. Lett.* **1998**, *291* 253–261. b) T. Nakabayashi, K. Kosugi, N. Nishi, *J. Phys. Chem. A* **1999**, *103*, 8595-8603.
17. a) H. Tokuda, K. Hayamizu, K. Ishii, Md. A. B. H. Susan, M. Watanabe, *J. Phys. Chem. B* **2004**, *108*, 16593-16600. b) H. Tokuda, K. Hayamizu, K. Ishii, Md. A. B. H. Susan, M. Watanabe, *J. Phys. Chem. B* **2005**, *109*, 6103-6110. c) H. Tokuda, K. Ishii, Md. A. B. H. Susan, S. Tsuzuki, K. Hayamizu, M. Watanabe, *J. Phys. Chem. B* **2006**, *110*, 2833-2839. d) H. Tokuda, S. Tsuzuki, Md. A. B. H. Susan, K. Hayamizu, M. Watanabe, *J. Phys. Chem. B* **2006**, *110*, 19593-19600. e) K. Ueno, H. Tokuda, M. Watanabe, *Phys. Chem. Chem. Phys.* **2010**, *12*, 1649-1658.

18. a) R. P. Bell, *Proc*. *Roy*. *Soc*. *London* **1936**, 154A; doi:10.1098/rspa.1936.0060. b) M. G. Evans, M. Polanyi, *Trans*. *Faraday Soc*. **1938**, *34*, 11–24.
19. a) K. Fumino, A. Wulf, R. Ludwig, *Angew*. *Chem*. *Int*. *Ed*. **2009**, *48*, 3184 –3186. b) A. Wulf, K. Fumino, R. Ludwig, *Angew*. *Chem*. *Int*. *Ed*. **2010**, *49*, 449 –453. c) C. Roth, T. Peppel, K. Fumino, M. Köckerling, R. Ludwig, *Angew*. *Chem*. *Int*. *Ed*. **2010**, *49*, 10221 –10224. d) T. Peppel, C. Roth, K. Fumino, D. Paschek, M. Köckerling, R. Ludwig, *Angew*. *Chem*. *Int*. *Ed*. **2011**, *50*, 6661 –6665. e) K. Fumino, T. Peppel, M. Geppert-Rybczyńska, D. H. Zaitsau, J. K Lehmann, S. P. Verevkin, M. Köckerling, R. Ludwig, *Phys*. *Chem*. *Chem*. *Phys*. **2011**, *13*, 14064–14075. f) K. Fumino, E. Reichert, K. Wittler, R. Hempelmann, R. Ludwig, *Angew*. *Chem*. *Int*. *Ed*. **2012**, *51*, 6236 –6240. g) K. Fumino, K. Wittler, R. Ludwig, *J*. *Phys*. *Chem*. *B* **2012**, **116**, 9507-9511. h) K. Fumino, V. Fossog, K. Wittler, R. Hempelmann, R. Ludwig, *Angew*. *Chem*. *Int*. *Ed*. **2013**, *52*, 2368 –2372.
20. a) D. A. Turton, T. Sonnleitner, A. Ortner, M. Walther, G. Hefter, K. R. Seddon, S. Stana, N. V. Plechkova, R. Buchner, *Faraday Discussions* **2012**, *154*, 145-153. b) R. Buchner, G. Hefter, *Phys*. *Chem*. *Chem*. *Phys*. **2009**, *11*, 8984-8999.
21. a) Y. Umebayashi, T. Fujimori, T. Sukizaki, M. Asada, K. Fujii, R. Kanzaki, S. Ishiguro, *J*. *Phys*. *Chem*. *A* **2005**, *109*, 8976-8982. b) K. Fujii, T. Fujimori, T. Takamuku, R. Kanzaki, Y. Umebayashi, S. Ishiguro, *J*. *Phys*. *Chem*. *B* **2006**, *110*, 8179-8183. c) Y. Umebayashi, T. Mitsugi, S. Fukuda, T. Fujimori, K. Fujii, R. Kanzaki, M. Takeuchi, S. Ishiguro, *J*. *Phys*. *Chem*. *B*, **2007**, *111*, 13028-13032. d) Y. Umebayashi, T. Yamaguchi, S. Fukuda, T. Mitsugi, M. Takeuchi, K. Fujii, S. Ishiguro, *Anal*. *Sci*., **2008**, *24*, 1297-1304. e) K. Fujii, T. Nonaka, Y. Akimoto, Y. Umebayashi, S. Ishiguro, *Anal*. *Sci*., **2008**, *24*, 1377-1380. f) Y. Umebayashi, T. MIstugi, K. Fujii, S. Seki, K. Chiba, H. Yamamoto, J. N. C. Lopes, A. A. H. Pádua, M. Takeuchi, R. Kanzaki, S. Ishiguro, *J*. *Phys*. *Chem*. *B*, **2009**, *113*, 4338–4346. g) Y. Umebayashi, S. Mori, K.

Fujii, S. Tsuzuki, S. Seki, K. Hayamizu, S. Ishiguro, *J. Phys. Chem. B*, **2010**, *114*, 6513-6521. h) Y. Umebayashi, H. Hamano, S. Tsuzuki, J. N. C. Lopes, A. A. H. Pádua, Y. Kameda, S. Kohara, T. Yamaguchi, K. Fujii, S. Ishiguro, *J. Phys. Chem. B*, **2010**, *114*, 11715-11724. i) Y. Umebayashi, H. Hamano, S. Seki, B. Minofar, K. Fujii, K. Hayamizu, S. Tsuzuki, Y. Kameda, S. Kohara, M. Watanabe, *J. Phys. Chem. B*, **2011**, *115*, 12179–12191.

22. M. J. Frisch, G. W. Trucks, H. B. Schlegel, G. E. Scuseria, M. A. Robb, J. R. Cheeseman, J. A. Montgomery, Jr., T. Vreven, K. N. Kudin, J. C. Burant, J. M. Millam, S. S. Iyengar, J. Tomasi, V. Barone, B. Mennucci, M. Cossi, G. Scalmani, N. Rega, G. A. Petersson, H. Nakatsuji, M. Hada, M. Ehara, K. Toyota, R. Fukuda, J. Hasegawa, M. Ishida, T. Nakajima, Y. Honda, O. Kitao, H. Nakai, M. Klene, X. Li, J. E. Knox, H. P. Hratchian, J. B. Cross, C. Adamo, J. Jaramillo, R. Gomperts, R. E. Stratmann, O. Yazyev, A. J. Austin, R. Cammi, C. Pomelli, J. W. Ochterski, P. Y. Ayala, K. Morokuma, G. A. Voth, P. Salvador, J. J. Dannenberg, V. G. Zakrzewski, S. Dapprich, A. D. Daniels, M. C. Strain, O. Farkas, D. K. Malick, A. D. Rabuck, K. Raghavachari, J. B. Foresman, J. V. Ortiz, Q. Cui, A. G. Baboul, S. Clifford, J. Cioslowski, B. B. Stefanov, G. Liu, A. Liashenko, P. Piskorz, I. Komaromi, R. L. Martin, D. J. Fox, T. Keith, M. A. Al-Laham, C. Y. Peng, A. Nanayakkara, M. Challacombe, P. M. W. Gill, B. Johnson, W. Chen, M. W. Wong, C. Gonzalez, and J. A. Pople, *Gaussian*, *Inc*., Wallingford CT, **2004**.

Chapter 4

Figures and Tables

A Novel Proton Conductive Liquid with No Ions: *Pseudo* Protic Ionic Liquids

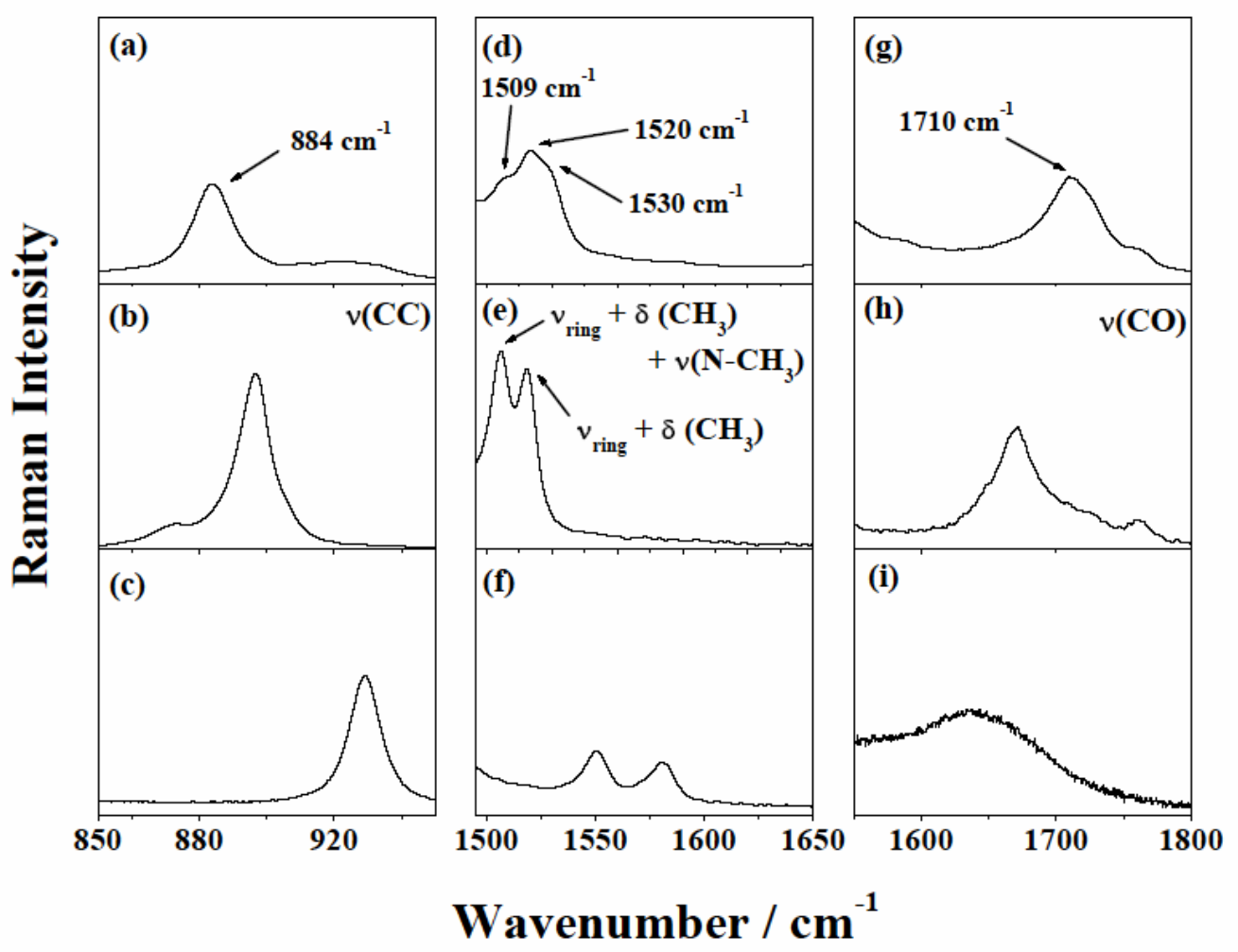

Figure 1. Raman spectra of (a), (g) C_1Im and AcOH mixture, (b), (h) neat acetic acid and (c), (i) 1 mol dm^{-3} sodium acetate aqueous solution in the frequency range of 850 - 950cm^{-1} for (a) - (c) and 1550 - 1800cm^{-1} for (g) - (i), respectively, and those of (d) the mixture, (e) neat C_1Im and (f) [C_1hIm^+][Cl^-] in the range of 1490 - 1650 cm^{-1}.

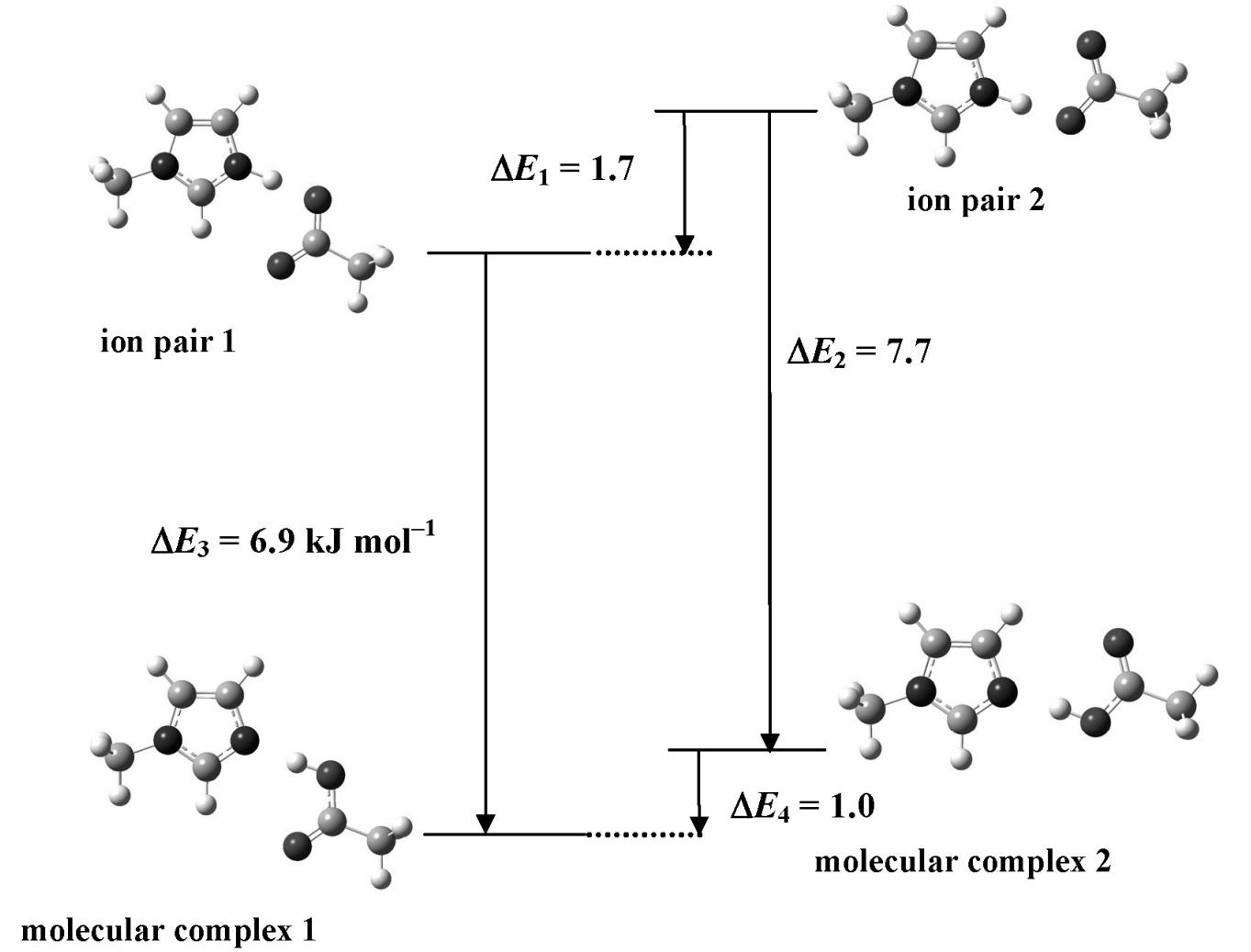

Figure 2. Energy levels for the ion pairs 1 and 2 and for the molecular complexes 1 and 2 in acetonitrile ($\varepsilon_r = 36.64$) with the PCM calculations at the B3LYP/6-311+G(d,p) level of theory accompanied by their optimized geometries.

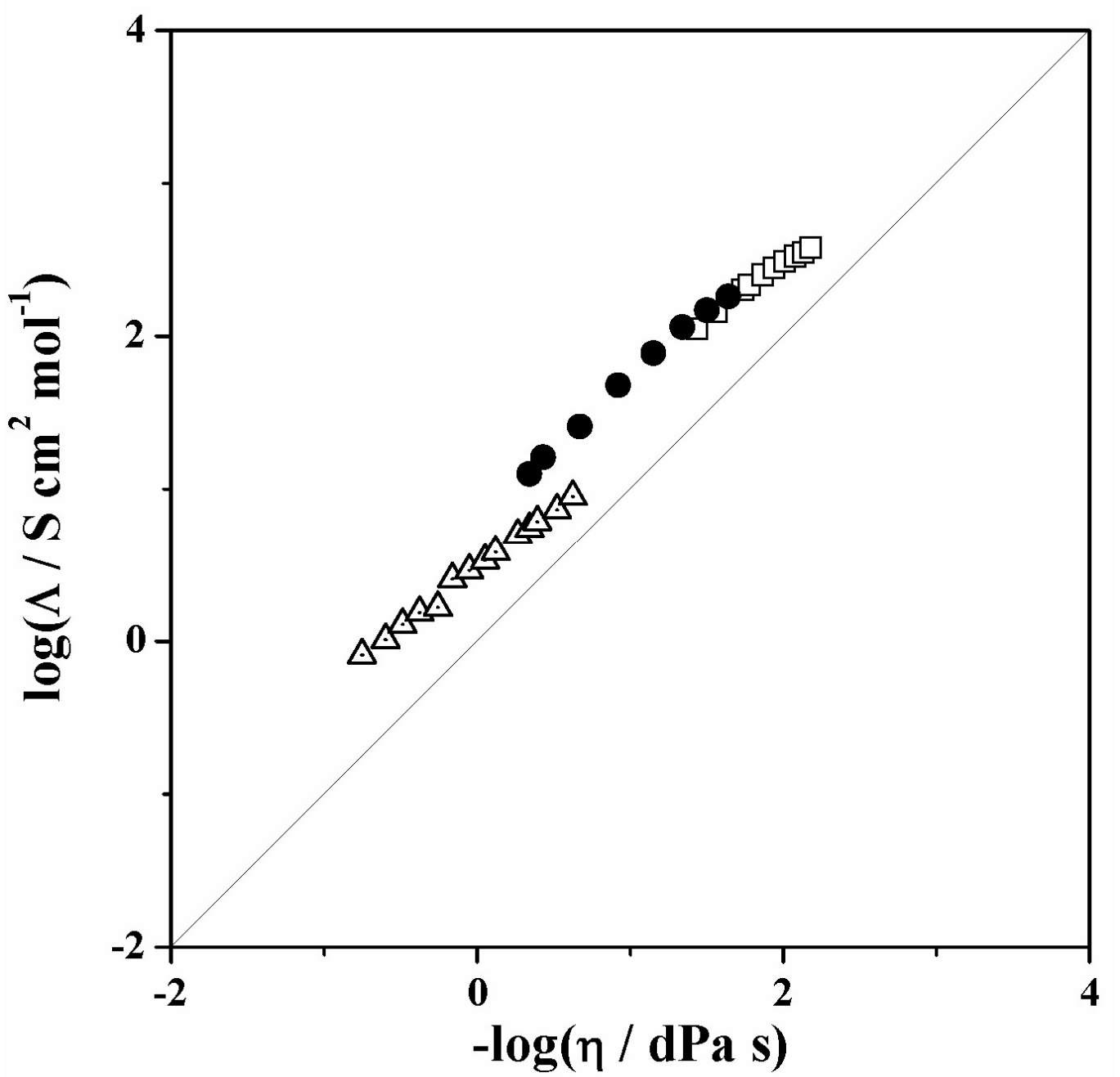

Figure 3. Walden plots for *N*-methylimidazole and acetic acid mixture at various temperatures (●) accompanied by 4 mol dm^{-3} sulfuric acid (□) and 98% phosphoric acid (△) for comparison.

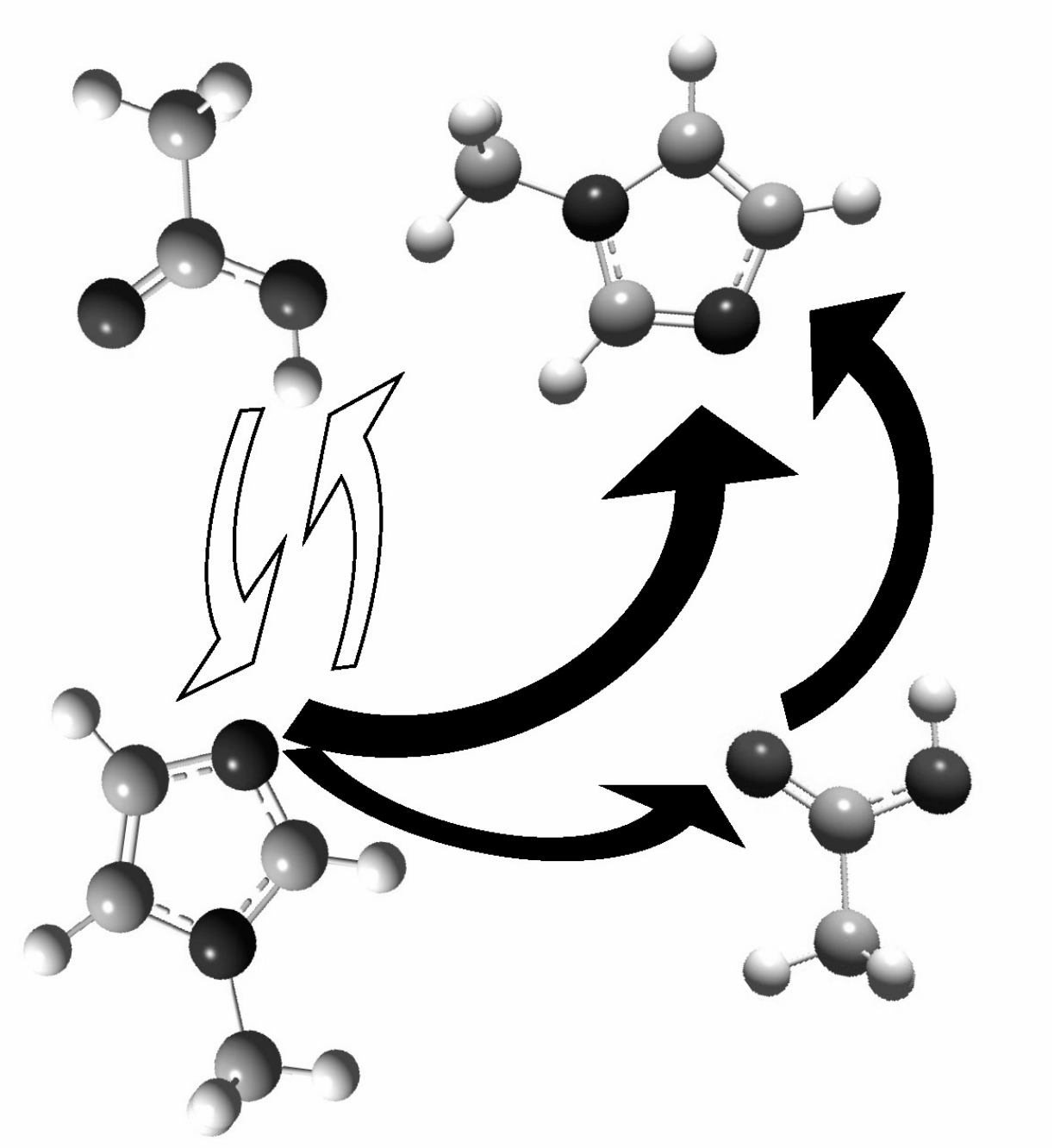

Figure 4. Possible proton conductive mechanism for the C_1Im and AcOH mixtures.

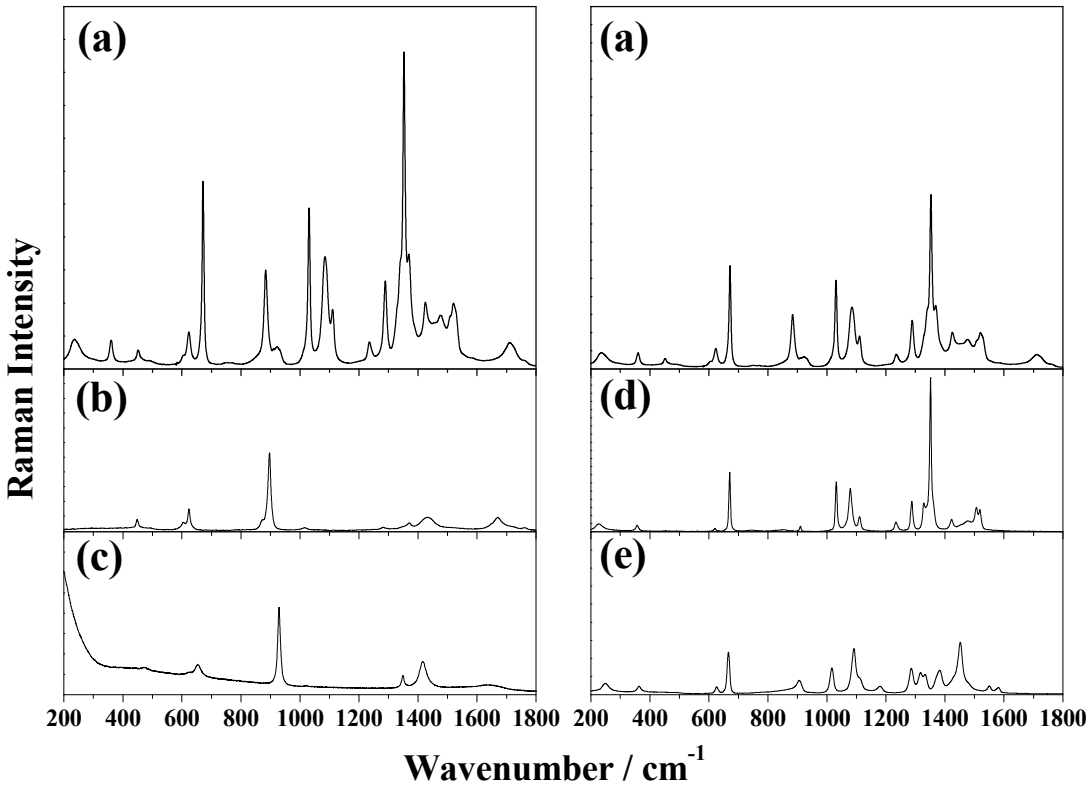

Figure 5 Raman spectra of (a), (d) C_1Im + AcOH mixture, (b) neat AcOH and (c) 1 mol dm^{-3} NaAcO aqueous solution, and those of (e) neat C_1Im and (f) $[C_1hIm^+][Cl^-]$ in the frequency range of 200 – 1800 cm^{-1}.

Table 1 Observed Raman bands for C_1Im and AcOH mixture, neat C_1Im, neat AcOH, $[C_1hIm^+][Cl^-]$ and 1 mol dm^{-3} NaAcO aqueous solution

C_1Im and AcOH mixture		C_1Im		neat AcOH		$[C_1hIm^+][Cl^-]$		acetate[a]	
ν / cm^{-1}	Int.	ν / cm^{-1}	Int.	ν / cm^{-1}	Int.	ν / cm^{-1}	Int.	ν / cm^{-1}	Int.
236.4	w	227.5	w			249.6	w		
247	w, sh								
360.2	w	357.0	w			363.2	w		
451.4	vw			448	m			473.2	vw
462.6	vw, sh								
604	vw, sh			604.8	w			622.5	vw
		620.4	vw			626.4	w		
623.4	w			623.8	m			653.6	w
671.6	s	670.5	s			666	vs		
				873.4	w, sh				
884	m			896.8	vs			929.6	s
929.5	w	910.5	vw			906.6	m		
1017	w, sh								
1031	s	1031.5	m			1016.8	s		
1084.8	m	1079.4	m			1091.6	vs		
1110.4	w	1110.5	w			1113	m, sh		
1235	w	1233.5	w						
1289.2	m	1288	m			1286.2	s		
						1317.6	m		
1340.2	s, sh	1328.4	m			1332.8	m		
								1348.8	m
1352.4	vs	1351	vs			1366	m, sh		
		1361.2	m, sh						
								1416	m
						1430	m, sh		
				1431.6	m, br				
1477.4	m	1477	w			1452.2	vs		
		1506.4	m						
1509	m, sh								
						1550.6	w		
1520	m	1518.5	m			1580.8	w		
1530	m, sh								
1710	w			1671.4	m			1640	w, br
				1707.8	vw, sh				
1724	w, sh								
1762	w, sh			1760.2	vw				

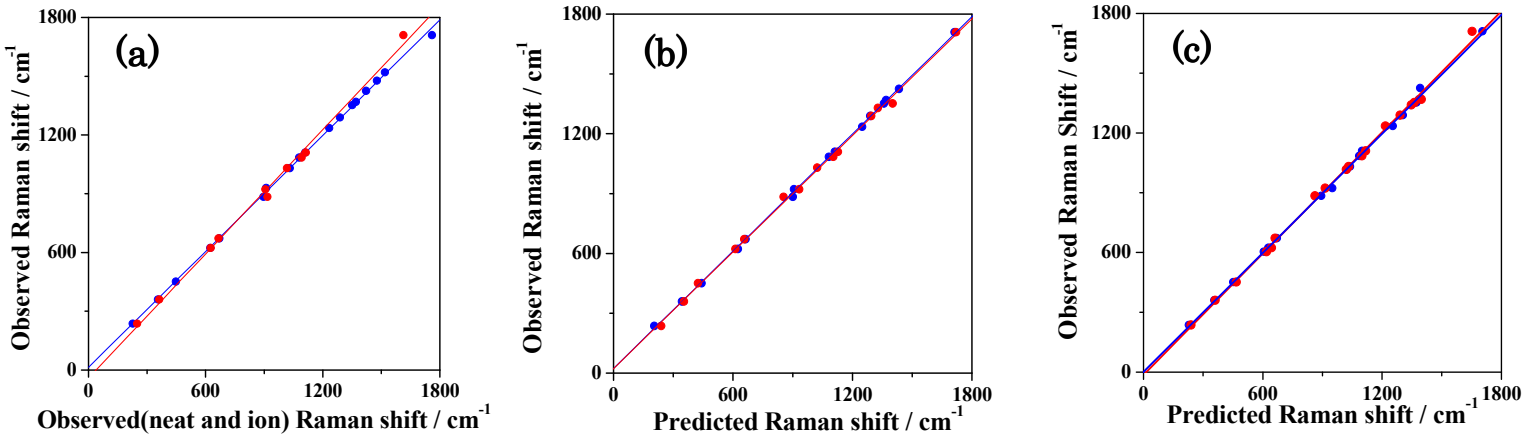

Figure.6 Plots of peak positions of observed Raman bands for the C_1Im and AcOH mixture vs. (a) those for neat C_1Im and neat AcOH (blue, y = 0.986(7)x + 14(8)) and those for $[C_1hIm^+][Cl^-]$ and 1 mol dm^{-3} NaAcO aqueous solution (red, y = 1.06(2)x - 40(20)), vs. (b) the predicted ones at the B3LYP/6–311+G(d, p) for the isolated C_1Im and AcOH cyclic dimer in gas phase (blue y = 0.980(4)x + 23(5)), and those for the isolated C_1hIm^+ and AcO^- ion in gas phase (red y = 0.97(1)x + 20(10)), and vs. (c) those predicted for the molecular complex 1 (blue y = 0.996(9)x + 1(9)) in acetonitrile (ε_r = 36.64) with the PCM calculation and those for the ion pair 1 (red y = 1.01(1)x - 10(20)).

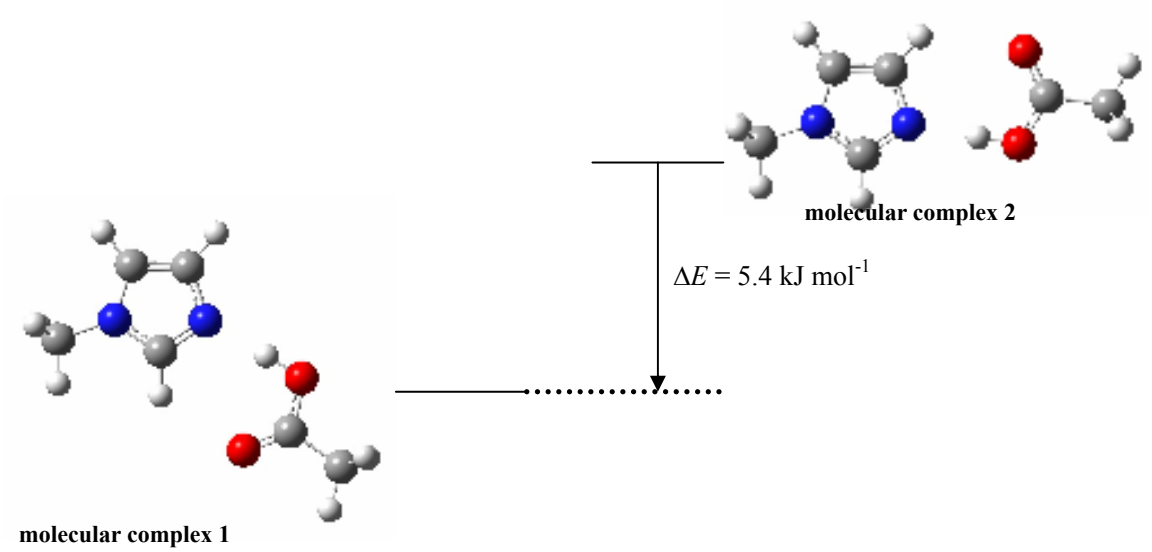

Figure.7 Energy level for the molecular complexes 1 and 2 in gas phase at the B3LYP/6-311+G(d,p) level of theory with the optimized geometries.

Table 2 Structural parameters for the molecular complexes 1 and 2 in gas phase and in acetonitrile, and the ion pairs 1 and 2 in acetonitrile at the B3LYP/6-311+G(d,p) level of theory.

	1			2		
	gas phase $\varepsilon_r = 1$	in acetonitrile $\varepsilon_r = 36.64$		gas phase $\varepsilon_r = 1$	in acetonitrile $\varepsilon_r = 36.64$	
	complex	complex	ion pair.	complex	complex	Ion pair
bond length / Å						
r(O-H)	1.01	1.03	1.48	1.00	1.03	1.47
r(N-H)	1.72	1.62	1.10	1.73	1.63	1.11
r(CH-O)	2.42	2.61	2.87	2.56	3.00	3.00
bond angle / degree						
O-H-N	177.1	176.8	178.3	179.3	174.9	179.5
C-H-O	123.1	115.7	113.4	123.9	114.7	115.9
energy / kJ mol^{-1}						
ΔE_b	-51.3	-31.9	-47.1	-46.6	-30.9	-45.3
BSSE	2.2	2.4	2.4	1.5	2.4	2.4

Table 3 Theoretical Raman bands for the molecular complexes 1 and 2 in gas phase and in acetonitrile, and the ion pairs 1 and 2 in acetonitrile at the B3LYP/6-311+G(d,p)
level of theory.

1						2					
gas phase		in acetonitrile				gas phase		in acetonitrile			
complex		complex		ion pair		complex		complex		ion pair	
ν / cm^{-1}	Int.	ν / cm^{-1}	Int.	ν / cm^{-1}	Int.	ν / cm^{-1}	Int.	ν / cm^{-1}	Int.	ν / cm^{-1}	Int.
34.3	0.2	32.6	0.3	32.1	0.3	26.9	0.2	25.6	0.5	36.6	0.2
37.8	1.1	33.4	0.02	34.7	1.2	49.5	0.9	36.7	0.6	54.4	1.2
56.9	0.05	45.9	2.2	37.9	0.2	55.1	0.7	46.8	0.3	63.6	0.2
60.5	0.2	57.7	0.9	53.3	1.3	60.7	0.3	58.9	0.3	66.7	0.04
76.9	0.5	78.4	0.7	65.1	0.4	82.9	1.0	76.9	1.2	69.5	0.6
102.3	1.1	111.8	4.0	109.2	2.6	123.9	0.8	111.2	0.3	108.9	1.9
112.3	0.04	125.5	0.2	112	0.04	125.6	4.8	121	2.5	127.4	0.3
168.5	0.1	170.2	0.6	173.9	0.5	176.5	0.3	174.6	0.5	167.3	0.2
218.3	1.5	228.2	3.3	230	3.8	239.5	2.9	241.9	3.7	215.9	1.1
356.4	0.5	356.3	1.9	355.9	1.6	360.6	2.0	360.3	1.9	357.7	0.9
447.1	0.7	451.5	2.1	452.1	2.1	466.8	1.2	468.9	1.1	449.1	0.7
600.1	0.9	605.1	1.8	605.2	1.5	618.7	2.1	618.1	2.0	602.6	0.9
623.2	0.4	628	6.6	626.9	5.7	635.5	0.5	633	0.5	625.9	0.2
625.2	4.1	630.4	0.7	629.9	0.7	643.2	10.3	642.2	11.6	627.0	4.9
667.6	0.09	667.8	0.3	668.6	0.4	643.7	0.8	644	0.8	669.3	0.1
678	9.4	670.9	10.7	671	12.4	661.7	13.8	660.1	16.4	677.8	6.6
735.8	1.7	754.5	7.6	755.7	6.4	754.4	3.1	759.1	3.0	732.5	1.5
815.4	0.3	845.8	1.4	835.4	0.9	862.5	18.3	844.6	0.9	860.5	1.1
887.8	13.5	872	6.5	879.8	6.4	864.3	8.7	857.7	25.1	875.6	0.7
907.5	1.2	894.1	20.8	893.2	21.1	877.1	4.3	886.8	5.5	891.0	12.5
937.3	1.6	950.1	4.6	948.2	4.7	913.6	29.2	913.1	28.5	941.7	1.8
1020.1	1.3	1022.3	2.3	1022.2	1.3	1020.4	1.9	1021.2	2.6	1023.3	1.5
1041.7	0.3	1039.2	18.0	1039.4	18.0	1031.5	17.6	1033.2	19.6	1039.1	11.6
1041.9	9.3	1061.1	0.8	1061.5	0.7	1055.5	0.6	1055.3	0.6	1052.6	0.3
1066	0.1	1085	4.9	1084.8	6.5	1089.7	5.1	1094.3	21.2	1067.3	0.2
1080.3	2.6	1099.4	27.5	1098.1	27.2	1098.6	34.1	1098.6	24.9	1078.2	4.3
1101.1	17.5	1104.6	0.1	1101.3	0.5	1117.5	8.9	1112	14.4	1101.3	10.0
1139.5	6.5	1123	10.3	1121.9	13.7	1150.2	0.5	1150	0.4	1138.2	4.9
1145.5	0.7	1146.8	0.5	1145.9	0.5	1201.4	1.4	1211.6	1.6	1145.9	0.7
1262.4	4.1	1253.8	13.1	1259.5	18.0	1216.7	31.6	1233.7	15.3	1262.2	7.2
1290.3	10.1	1288	12.9	1286.3	8.4	1290.8	32.0	1285.5	55.5	1301.9	4.5
1306.5	6.9	1304.2	22.8	1303.8	25.3	1346.6	21.8	1337.5	36.5	1307.5	8.1
1383.2	42.5	1372.7	89.1	1372	87.1	1362.1	61.6	1360.6	37.7	1380.6	21.0
1385.7	2.3	1385.9	49.2	1385.1	51.7	1391.7	14.5	1390.3	8.4	1386.1	26.4
1394.3	2.3	1391.4	14.5	1390.4	5.7	1397.7	45.4	1398.9	46.9	1397.6	6.5
1454.3	5.9	1448.3	17.5	1448.4	13.2	1450.4	23.4	1450.2	26.9	1452.6	7.2
1468.4	6.3	1453.4	21.0	1454.5	19.8	1453	15.6	1453.1	12.2	1470.3	9.2
1478.2	7.1	1462.6	14.0	1462.3	13.9	1467.7	15.2	1468	14.9	1478.9	7.0
1482.3	5.0	1475	18.4	1474.6	17.4	1475.7	16.7	1474.4	16.4	1487.9	8.8
1487.6	9.4	1497	38.2	1494.1	24.8	1497.7	39.4	1496.1	43.5	1491.6	6.3
1514.3	13.3	1506.8	11.7	1500.6	20.3	1532.6	38.8	1530.8	48.0	1512.7	14.7
1544	2.5	1541.2	2.7	1540.3	1.7	1562.2	17.9	1554.4	13.9	1538.9	3.3
1552.3	8.1	1557.3	29.1	1556.6	27.1	1577	17.1	1581.2	8.6	1551.2	13.5
1769.8	10.5	1704.5	28.8	1707.3	29.5	1653.1	13.9	1662.9	7.7	1762.4	10.4
3029.9	291.3	2558.6	490.9	2600.8	532.8	2089.3	256.8	2039.7	250.6	2975.3	334.2
3043.8	280.5	3043.4	319.4	3044.4	314.4	3035.4	322.2	3035.1	321.5	3043.0	204.4
3046.4	194.4	3048.9	348.9	3048.7	348.5	3058.2	334.3	3058.4	342.4	3047.4	170.6
3104.9	91.4	3106.6	120.4	3106.4	116.0	3096	122.9	3096	122.4	3104.2	87.9
3105.2	60.2	3121.7	150.1	3121	149.5	3128.4	122.3	3127.7	125.1	3106.4	63.5
3134.8	53.6	3147	105.6	3146.8	107.3	3137.7	134.4	3137.4	136.0	3138.2	48.0
3151.1	56.8	3149.4	107.0	3150.4	103.6	3159.3	101.3	3160.1	101.9	3151.9	55.6
3246	54.1	3245.7	113.6	3249.5	59.7	3271.6	91.9	3273.8	77.8	3246.9	60.2
3252.1	46.6	3256.9	87.6	3251.2	149.2	3281.4	44.4	3278.2	81.5	3248.8	42.5
3271.2	127.8	3269.7	240.3	3270.8	220.5	3287.6	262.4	3290	227.0	3269.6	149.7

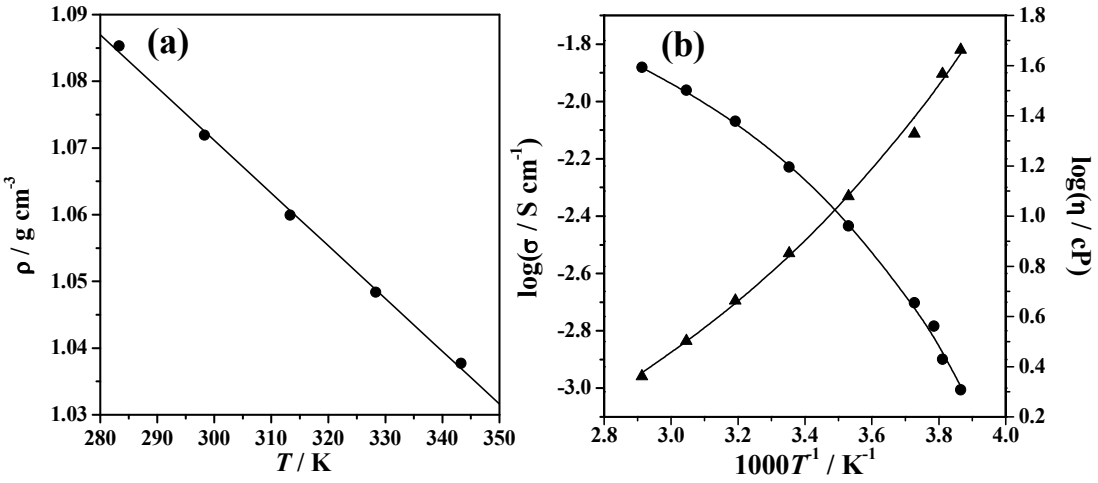

Figure.8 Temperature dependence of (a) the density (ρ = -7.9(2)×10^{-4}T + 1.308(6)), and the VTF plots for (b) ionic conductivity (●) and viscosity (▲) for the C_1Im + AcOH mixture.

Table.4 The VTF parameters for the ionic conductivity ($\sigma = AT^{-1/2} \exp[-B/(T-T_0)]$) and the viscosity($\eta = AT^{1/2}\exp[B/(T-T_0)]$

	A / Scm^{-1} K$^{1/2}$	B / K	T_0 / K
σ	1.46	252	203
η	5.00 × 10^{-3}	564	169

Chapter 5

Conclusion

In order to investigate acid-base reaction mechanisms in protic ionic liquids, thermodynamic quantities of a proton transfer reaction in a series of protic ionic liquids made from *N*-methylimidazole and five acids with a wide variety of acidities from strong acids to weak ones were determined by direct potentiometric and calorimetric titrations. We demonstrated that the acidity of two widely used strong acids, trifluoromethanesulfonic acid and bis-(trifluromethanesulfonyl)amide, are practically similar in these protic ionic liquids, and that the acidity of trifluoroacetic acid is much weaker than trifluoromethanesulfonic acid and bis-(trifluromethanesulfonyl)amide. In addition, we found that the mixtures of *N*-methylimidazole and acetic acid and formic acid are not essentially ionic liquids.

For further insight into ion conduction in *N*-methylimidazole equimolar mixute with acetic acid, ionic conductivity, viscosity and density were investigated at various temperatures. In addition, Raman spectroscopic study and quantum calculations were performed to reveal predominant species in the mixture; ions of *N*-methylimidazolium cation and acetate anion or electrically neutral molecules of *N*-methylimidazole molecule and acetic acid molecule. We found that ionic species are practically negligible in the mixture. Taking it into consideration, the Walden plots for the mixture located upper region of the ideal Walden line proposed by Angell. This suggests specific proton conduction could occur in the mixture.

Acknowledgment

The author wishes to express deepest gratitude to Prof. Dr. Yasuhiro Umebayashi, Niigata Univ., who suggested the subject matter of this study and helped the author to achieve better understanding on the science of ionic liquid through many extensive discussions.

The author wishes to express his sincere thanks to Prof. Dr. Toshiyuki Takamuku, Vice Prof. Dr. Ryo Kanzaki, Dr. Babak Minofar, Dr. Xuedan Song and Vice Prof. Dr. Kenta Fujii for their helpful many advises and strong supports on this study.

The author also express his thank to the members of Solution Chemistry laboratory, Niigata Univ.

Part of doctoral work was supported by JSPS KAKENHI Grant Number 26・4098.

Lastly, the author wishes to express his sincere and deepest gratitude to his parents who gave him a chance for further education, supported and encouraged him throughout this study.

List of publications

1. *"Acid-base Property of N-methylimidazolium-based Protic Ionic Depending on Anion ",* Ryo Kanzaki, Hiroyuki Doi, Xuedan Song, Shota Hara, Shin-ichi Ishiguro and Yasuhiro Umebayashi. *J. Phys. Chem. B*, **2012**, *116*, 14146-14152.

2. *"A New Proton Conductive Liquid with No Ions: Pseudo-Protic Ionic Liquids"* Hiroyuki Doi, Xuedan Song, Babak Minofar, Ryo Kanzaki, Toshiyuki Takamuku and YasuhiroUmebayashi. *Chem. Eur. J.*, **2013**, *19*, 11522 – 11526

3. *"Unusual Li+ Ion Solvation Structure in Bis(fluorosulfonyl)amide Based Ionic Liquid"*, Kenta Fujii, Hiroshi Hamano, Hiroyuki Doi, Xuedan Song, Seiji Tsuzuki, Kikuko Hayamizu, Shiro Seki, Yasuo Kameda, Kaoru Dokko, Masayoshi Watanabe and Yasuhiro Umebayashi,
   J. Phys. Chem. C, **2013**, *117*, 19314−19324

4. *"High-Energy X-ray Diffraction and MD Simulation Study on the Ion-Ion Interactions in 1-Ethyl-3-methylimidazolium Bis(fluorosulfonyl)amide"*, Kenta Fujii, Shiro Seki, Koji Ohara, Yasuo Kameda, Hiroyuki Doi, Soshi Saito and Yasuhiro Umebayashi,
   J. Solution Chem, **2014**, **43**, 1655-1668

5. *"Conformation of ATP and ADP Molecules in Aqueous Solutions Determined by Highenergy X-ray Diffraction"*, Takuya Miyazaki, Yasuo Kameda, Yasuhiro Umebayashi, Hiroyuki Doi, Yuko Amo, Takeshi Usuki,
   J. Solution Chem, **2014**, *43*, 1487–1498

6. *"Static and Transport Properties of Alkyltrimethylammonium Cation-Based Room-Temperature Ionic Liquids"*, Shiro Seki, Seiji Tsuzuki, Kikuko Hayamizu, Nobuyuki Serizawa, Shimpei Ono, Katsuhito Takei, Hiroyuki Doi, and Yasuhiro Umebayashi,

J. Phys. Chem. B, **2014**, *118*, 4590−4599

7. "次世代蓄電・発電デバイス電解液のスペシエーション分析

: 分光熱力学 ― イオン液体中のリチウムイオン溶媒和―",

梅林泰宏, 藤井健太, 齊藤蒼思, 渡辺日香里, 土井寛之,

分析化学, 64 巻, 3 号, 197-202 頁, **2015**.

8. *"Structural and aggregate analyses of (Li salt + glyme) mixtures: the complex nature of solvate ionic liquids"*, Karina Shimizu, Adilson A. Freitas, Rob Atkin, Gregory G. Warr, Paul A. FitzGerald, Hiroyuki Doi, Soshi Saito, Kazuhide Ueno, Yasuhiro Umebayashi, Masayoshi Watanabe and Jose N. Canongia Lopes,
Phys. Chem. Chem. Phys., **2015**, *17*, 22321-22335

9. *"Li^+ solvation in glyme–Li salt solvate ionic liquids"*, Kazuhide Ueno, Ryoichi Tatara, Seiji Tsuzuki, Soshi Saito, Hiroyuki Doi, Kazuki Yoshida, Toshihiko Mandai, Masaru Matsugami, Yasuhiro Umebayashi, Kaoru Dokko and Masayoshi Watanabe*
Phys. Chem. Chem. Phys., **2015**, *17*, 8248-8257

10. *"Hydrogen bond in imidazolium based protic and aprotic ionic liquids"*, Hikari Watanabe, Hiroyuki Doi, Soshi Saito, Masaru Matsugami, Kenta Fujii, Ryo Kanzaki, Yasuo Kameda and Yasuhiro Umebayashi,
J. Mol. Liq., **2015**, Article In Press.

List of presentation at international conferences

Oral (6)

1. Possibility of Super Arrhenius proton Conduction in *pseudo*-Protic Ionic Liquids: imidazole and acetic acid equimolar mixture
   Yasuhiro Umebayashi, Hikari Watanabe, Tatsuya Umecky, Hiroyuki Doi, Soshi Saito, Kenta Fujii, Toshiyuki Takamuku and Yasuo Kameda
   Rostock, Germany, Joint EMLG/JMLG Annual Meeting 2015, Sep. 6^{th}-10^{th}, 2015

2. Lithium Ion Solvation in Room-temperature Ionic Liquids toward Next Generation Batteries Based on Spectrothermodynamics,
   Yasuhiro Umebayashi, Kenta Fujii, Hiroyuki Doi, Soshi Saito, Hikari Watanabe, Shiro Seki, Seiji Tsuzuki, Yasuo Kameda,
   Invited talk, 34^{th} International Conference on Solution Chemistry 2015, Prague, Czech Republic, Aug. 30th -Sep. 3^{rd}, 2015

3. Possibility of super Arrhenius ion conduction : *pseudo*-protic ionic liquids,
   Yasuhiro Umebayashi, Hiroyuki Doi, Hikari Watanabe, Thomas Sonneleitner, Richard Buchner, Yuko Amo,
   Invited talk, 248th ACS National Meeting, August 10-14, 2014, San Francisco, CA, United States

4. Structure and dynamics of pseudo-protic ionic liquids as novel proton conductors
   Hiroyuki Doi, Xuedan Song, Kenta Fujii, Ryo Kanzaki, Takuya Miyazaki, Yasuo Kameda, and Yasuhiro Umebayashi
   Invited talk, Tokyo, Japan, Post-symposium on Ionic Liquids From Science to Green Chemical Applications at 33rd International Conference on Solution Chemistry 33ICSC, July 13, 2013

5. Possibility of specific proton conduction in *N*-methylimidazole-acetic acid equimolar mixture,
   Hiroyuki Doi, Xuedan Song, Kenta. Fujii, Ryo Kanzaki, Takuya Miyazaki, Yasuo Kameda, and Yasuhiro Umebayashi
   Kyoto, Japan, 33rd International Conference on Solution Chemistry 33ICSC, July 7th-12th, 2013

6. Closest ion-ion interaction and structural heterogeneity of 1-alkylimidazolium based protic ionic liquids
   Yasuhiro Umebayashi, Hiroshi Hamano, Hiroyuki Doi, Xuedan. Song, Ryo Kanzaki, Kenta Fujii, Yasuo Kameda
   Algarve, Portugal, 5th congress on ionic liquids, April 21st-25th, 2013

Poster (9)

1. High energy X-ray scattering studies on liquid structure of pseudo-Protic Ionic Liquid *N*-methylimidazole and actic acid equimolar mixture with the aids of MD simulations,
   Hiroyuki Doi, Hikari Watanabe, Thomas Sonnleitner, Andreas Nazet, Soshi Saito, Kenta Fujii, Tatsuya Umecky, Toshiyuki Takamuku, Yasuo Kameda, Richard Buchner and Yasuhiro Umebayashi
   Rostock, Germany, Joint EMLG/JMLG Annual Meeting 2015, Sep. 6th-10th, 2015

2. Possible proton conduction mechanism in *N*-methylimidazole and acetic acid equimolar mixture; the pseudo-protic ionic liquid,
   Hiroyuki Doi, Hikari Watanabe, Thomas Sonnleitner, Soshi Saito, Kenta Fujii, Tatsuya Umecky, Toshiyuki Takamuku, Yasuo Kameda, Richard Buchner and Yasuhiro Umebayashi,
   Prague, Czech Republic, 34th International Conference on Solution Chemistry 2015, Aug. 30th – Sep. 3rd, 2015

3. Dynamics of protic and *pseudo*-protic ionic liquids,
   Thomas Sonnleitner, Hiroyuki Doi, Yasuhiro Umebayashi, Andreas Nazet, Richard Buchner,
   Tallinn, Estonia, EUCHEM2014, July 6th-11th, 2014

4. Li^+ ion speciation in Li-glymes ionic liquids toward rechargeable batteries
   Soshi Saito, Hiroyuki Doi, Toshihiko Mandai, Kazuhide Ueno, Seiji Tsuzuki, Wataru Shinoda, Shiro Seki, Kaoru Dokko, Masayoshi Watanabe, and Yasuhiro Umebayashi
   Tokyo, Japan, Post-symposium on Ionic Liquids From Science to Green Chemical Applications at 33rd International Conference on Solution Chemistry 33ICSC, July 13, 2013

5. Liquid and Li^+ Local Structures in Li-glymes Complex Ionic Liquids Revealed by Raman and X-ray Scattering Techniques with the Aid of Theoretical Calculations
   Soshi Saito, Hiroyuki Doi, Seiji Tsuzuki, Wataru Shinoda, Shiro Seki, Kaoru Dokko, Masayoshi Watanabe, and Yasuhiro Umebayashi
   Kyoto, Japan, 33rd International Conference on Solution Chemistry 33ICSC, July 7^{th}-12^{th}, 2013

6. Raman spectroscopic study on *N*-methylimidazolium based Protic Ionic Liquids
   Hiroyuki Doi, Xuedan Song and Yasuhiro Umebayashi
   32nd International Conference on Solution Chemistry 32ICSC, Montpellier, France, Aug. 28^{th}-Sep.2^{nd}, 2011

7. Dielectric Relaxation spectroscopic speciation analysis of *N*-methylimidazole equimolar mixture with acetic acid,
   Hiroyuki Doi, Thomas Sonnleitner, Hikari Watanabe, Soshi Saito, Richard Buchner, Yasuhiro Umebayashi
   Chiba, Japan, RSC Tokyo International Conference 2014, September 4-5, 2014

8. Speciation and structure analysis of Li^+ in the Li -glyme solvate ionic liquids as new electrolytes for next generation lithium batteries.
   Soshi Saito, Hiroyuki Doi, Hikari Watanabe, Seiji Tsuzuki, Shiro Seki, Kaoru Dokko, Masayoshi Watanabe, Yasuhiro Umebayashi
   Chiba, Japan, RSC Tokyo International Conference 2014, September 4-5, 2014

9. Raman and NMR spectroscopic speciation analysis of proton carrier in imidazole and acetic acid equimolar mixture as *pseudo*-protic ionic liquids of new proton conductors,
   Hikari Watanabe, Tatsuya Umecky, Hiroyuki Doi, Soshi Saito, Ryo Kanzaki, Toshiyuki Takamuku, Yasuhiro Umebayashi
   Chiba, Japan, RSC Tokyo International Conference 2014, September 4-5, 2014